CHAPTER THREE

Structure and Function of Endoplasmic Reticulum STIM Calcium Sensors

Peter B. Stathopulos[1], Mitsuhiko Ikura[1]
Department of Medical Biophysics and Ontario Cancer Institute, University of Toronto and University Health Network, Toronto, Ontario, Canada
[1]Corresponding authors: e-mail address: pstathop@uhnres.utoronto.ca; mikura@uhnres.utoronto.ca

Contents

Abstract

Store-operated calcium (Ca^{2+}) entry (SOCE) is a vital Ca^{2+} signaling pathway in nonexcitable as well as electrically excitable cells, regulating countless physiological and pathophysiological pathways. Stromal interaction molecules (STIMs) are the principal regulating molecules of SOCE, sensing changes in sarco-/endoplasmic reticulum (S/ER) luminal Ca^{2+} levels and directly interacting with the Orai channel subunits to orchestrate the opening of Ca^{2+} release-activated Ca^{2+} (CRAC) channels. Recent atomic resolution structures on human STIM1 and STIM2 have illuminated critical mechanisms of STIM function in SOCE; further, the first high-resolution structure of the *Drosophila melanogaster* Orai channel has revealed vital data on the atomic composition of the CRAC channel pore and the assembly of individual Orai subunits. This chapter focuses on the mechanistic information garnered from these high-resolution structures and the supporting biophysical, biochemical, and live cell work that has enhanced our understanding of the relationship between STIM and Orai structural features and CRAC channel function.

Current Topics in Membranes, Volume 71
ISSN 1063-5823
http://dx.doi.org/10.1016/B978-0-12-407870-3.00003-2

1. INTRODUCTION

Extracellular stimuli which interact with receptors on the surface of eukaryotic cells initiate signaling cascades that control myriad cellular processes (Berridge, Lipp, & Bootman, 2000; Bootman & Lipp, 2001). For example, upon T-cell receptor or G-protein-coupled receptor agonist binding, phospholipases are either indirectly or directly activated resulting in the metabolism of phosphatidylinositol 4,5-bisphosphate (PIP_2), generating inositol 1,4,5-trisphospate (IP_3) and diacylglycerol (Berridge, Bootman, & Roderick, 2003; Bootman et al., 2001). The IP_3 molecule is a small diffusible messenger which directly binds to IP_3 receptors (IP_3Rs) on the cytosolic face of the endoplasmic reticulum (ER) membrane. Furthermore, IP_3 binding to IP_3Rs induces a conformational change on these enormous tetrameric Ca^{2+} release channels resulting in the opening of the IP_3R pore which permeates Ca^{2+} ions down a large concentration gradient from the relatively high Ca^{2+} levels of the ER lumen (i.e., ~100–800 μM) into the low free Ca^{2+} levels of the cytosol (i.e., ~0.1–1 μM) (reviewed in Stathopulos et al., 2012). Due to the high Ca^{2+} levels of the ER lumen compared to other intracellular compartments, this cellular partition is often termed the ER Ca^{2+} store. This intracellular Ca^{2+} release channel efflux into the cytosol can be terminated by release of the IP_3 molecule as well as a feedback mechanism by which Ca^{2+} binds to the IP_3R, thereby closing the channel. Interestingly, low levels of cytosolic Ca^{2+} increase the open probability, whereas high Ca^{2+} levels decrease the open probability, generating a bell-shaped Ca^{2+}-dependency in channel activity (reviewed in Stathopulos et al., 2012). While IP_3Rs are also found in electrically excitable cells, ryanodine receptors (RyRs) dominate intracellular Ca^{2+} release channel function in these cell types (reviewed in Van Petegem, 2012). Native RyRs do not bind IP_3, but can be activated by Ca^{2+} or cyclic adenosine diphosphate ribose; however, they share a remarkable structural and functional conservation in Ca^{2+} release channel function. For example, RyRs demonstrate a bell-shaped Ca^{2+}-dependency, and key domains within IP_3Rs and RyRs are interchangeable with a preservation of function suggesting a highly conserved activation mechanism exists between these two Ca^{2+} release channel cousins (Seo et al., 2012).

Ultimately, both RyRs and IP_3Rs regulate cytosolic and luminal Ca^{2+} levels. The spatial and temporal changes in intracellular Ca^{2+} mediate myriad physiological and pathophysiological activities in cells such as memory,

contraction, the immune response, and apoptosis, to name a few (Berridge et al., 2000). However, the sarco/ER (S/ER) lumen is only a limited source of Ca^{2+} as evidenced by S/ER Ca^{2+} ATPase (SERCA) pump blockers such as thapsigargin (TG) used in conjunction with fluorescent cytosolic Ca^{2+} indicators such as Fura-2 which demonstrate the exhaustible escape of Ca^{2+} from the lumen into the cytosol through leak pathways (Jackson, Patterson, Thastrup, & Hanley, 1988; Liou et al., 2005). While local and acute increases in cytosolic Ca^{2+} can trigger many processes, numerous cellular activities rely on longer, sustained cytosolic Ca^{2+} increases to elicit the signaling response, such as in transcriptional activation (reviewed in Hogan, Chen, Nardone, & Rao, 2003). Eukaryotic cells have evolved the intercompartmental coordination of Ca^{2+} signals to achieve the vast array of different activities required in life and death processes.

The major Ca^{2+} entry pathway of nonexcitable cells such as immune cells and platelets is store-operated calcium (Ca^{2+}) entry (SOCE) (Shaw & Feske, 2012; Varga-Szabo, Braun, & Nieswandt, 2011). SOCE is the process by which an external cell stimulus results in compartmentalized S/ER luminal Ca^{2+} release, through the IP_3-mediated pathway, for example; furthermore, this S/ER Ca^{2+} store release results in a communication between the Ca^{2+}-depleted S/ER lumen and the plasma membrane (PM). Subsequently, PM-resident Ca^{2+} channels open and Ca^{2+} enters the cytosol down a steep Ca^{2+} concentration gradient from the extracellular space (i.e., [Ca^{2+}] of the extracellular space ~1000 μM vs. ~0.1–1 μM in the cytosol) (Feske, 2007). The essentially inexhaustible supply of Ca^{2+} from the extracellular space has the capacity to provide a sustained Ca^{2+} entry required for longer term increases in cytosolic Ca^{2+}. Additionally, Ca^{2+} entering the cytosol via SOCE is an important source of Ca^{2+} for the SERCA pump refilling of the S/ER lumen. As critical Ca^{2+}-dependent processes take place within the S/ER lumen such as protein folding, chaperone quality control of protein folding, steroidogenesis, vesicle trafficking, and initiation of cell death pathways, it is essential that Ca^{2+} levels within the S/ER lumen do not remain chronically low (Berridge, 2002). Hence, SOCE provides the Ca^{2+} necessary to regulate cellular activities which require sustained elevation of cytosolic Ca^{2+} and to prevent Ca^{2+} levels of the S/ER lumen from becoming detrimentally low.

Although the SOCE model was first proposed in 1986 (Putney, 1986), almost two decades passed prior to the identification of the principal molecular players in this process. Using a systems biology approach which employed small inhibiting RNA (siRNA) knockdown of over 2300 human

genes, stromal interaction molecule-1 (STIM1) and -2 (STIM2) were identified as molecular components of SOCE (Liou et al., 2005). The genes were chosen based on the presence of primary sequence-identified signaling domains, and the level of SOCE activity was assessed in siRNA-transfected mammalian cells by monitoring changes in Fura-2 fluorescence after histamine and TG treatment which empty S/ER luminal Ca^{2+} stores via receptor-mediated IP_3 production and SERCA pump inhibition, respectively. In an independent study using an RNA interference (RNAi) screen of *Drosophila melanogaster* genes in S2 cells, knockdown of *D. melanogaster* STIM was identified to almost completely abolish an electrophysiological inward rectifying current with characteristics identical to mammalian T-cell Ca^{2+} release-activated Ca^{2+} (CRAC) current; furthermore, SOCE through CRAC channels is the principal Ca^{2+} entry pathway in human immune cells such as T-cells, and RNAi knockdown of the human homologue to *D. melanogaster*, STIM1 in human T-cells resulted in suppression of CRAC currents, thereby confirming STIM as a key molecular component of CRAC channels (Roos et al., 2005). Importantly, it was shown that mutation of key Ca^{2+} coordinating residues in the putative EF-hand resulted in constitutive CRAC activation, linking the a Ca^{2+} sensing ability of STIM to SOCE regulation (Zhang et al., 2005).

Interestingly, while STIM knockdown using inhibiting nucleic acid strategies suppressed SOCE, overexpression of STIM in mammalian cells only modestly increased SOCE activity (Liou et al., 2005; Roos et al., 2005). One year after the STIM molecular link was elucidated, a pedigree and interference RNA analysis identified another protein, Orai1 as critical in SOCE (Feske et al., 2006). A mutation in Orai1 (Arg91Trp), a predicted four-transmembrane (TM) protein, caused an inheritable form of severe combined immunodeficiency disease (SCID) in which patient T-cells showed a complete lack of CRAC entry (Feske et al., 2006). SCID was sensationalized in the late 1970s and early 1980s with reports of a SCID patient which spent the first 12 years of his life in isolation due to poor immune function (Lawrence, 1985; Stone, 1977). The identification of Orai1 as a key player in SOCE lead to studies showing that cooverexpression of STIM1 and Orai1 induces robust and dramatic increases in cytosolic Ca^{2+} after ER luminal Ca^{2+} depletion by TG (Mercer et al., 2006; Soboloff et al., 2006). Ultimately, studies confirmed that Orai1 was a subunit of the PM CRAC channel pore and a major molecular component of SOCE (Prakriya et al., 2006; Vig, Beck, et al., 2006; Vig, Peinelt, et al., 2006; Yeromin et al., 2006; Zhang et al., 2006). Prior to the identification of

the PM Orai proteins, the transient receptor potential family of proteins were candidates as the PM channels mediating SOCE (Draber & Draberova, 2005; Parekh & Penner, 1997; Parekh & Putney, 2005; Varga-Szabo, Braun, & Nieswandt, 2009).

Elucidation of three-dimensional (3D), atomic resolution protein structure is vital to understanding the precise mechanisms by which proteins function. In recent years, tremendous progress has been made in revealing high-resolution structural information on important conserved regions of STIM1 and Orai; further, combined with live cell experiments assessing SOCE in mammalian cells, great strides have been made in understanding the mechanisms of CRAC channel regulation and function. This chapter discusses the current known structural information of the CRAC components, with a particular emphasis on the mechanisms by which STIM molecules regulate Orai1 channel formation. Additionally, known structural differences between human STIM1 and STIM2 and how the distinctions and similarities relate to the discrete role of these homologues in mammalian cell signaling are discussed.

2. STIM AND Orai DOMAIN ARCHITECTURES

STIMs are single-pass TM proteins (Cai, 2007a). A small fraction of these proteins is localized to the PM after glycosylation of Asn131 and Asn171, while the vast majority is localized to the ER membrane where the function of these regulatory molecules is best understood (Manji et al., 2000; Williams et al., 2001, 2002; Zhang et al., 2005). Vertebrates express two homologues, STIM1 and STIM2. The sequence-identifiable ER luminal domains consist of an EF-hand and sterile α-motif (SAM) domains. The cytosolic portion of STIMs contains three conserved coiled-coil (CC) domains. Immediately proximal to the TM region a long CC1 is predicted followed by two shorter CC domains (i.e., CC2 and CC3) close in sequence space; further, the carboxy-terminal region of STIMs contain Pro/Ser-rich and poly-Lys regions (Fig. 3.1A). Homologues from lower to higher eukaryotes show conservation in these aforementioned domains (Cai, 2007a), which play crucial roles in the mechanisms of SOCE activation (see below). Human STIM1 and STIM2 share a 76% sequence similarity through a 558-amino acid overlap, analyzed using the Lalign server (Huang & Miller, 1991) (Fig. 3.1B). Nevertheless, these homologues play distinct roles in Ca^{2+} homeostasis and signaling. STIM1, which has been the focus of most of the research on this system to date, regulates

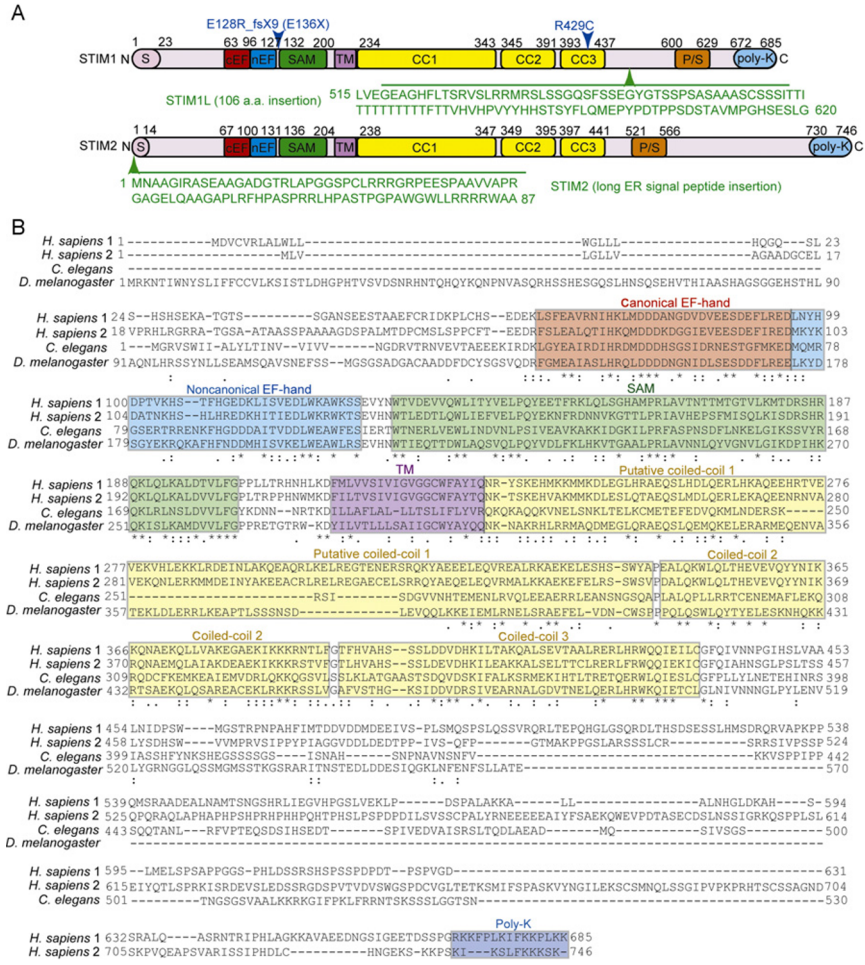

Figure 3.1 Domain architectures and sequence alignments of STIM proteins. (A) The architectures of the two *Homo sapiens* homologues, STIM1 and STIM2, are shown. S, signal peptide; cEF, canonical EF-hand; nEF, noncanonical EF-hand; SAM, sterile α-motif; TM, transmembrane region; CC1, putative coiled-coil 1; CC2, coiled-coil 2; CC3, coiled-coil 3; P/S, Pro/Ser-rich region; poly-K, Lys-rich region; N, amino terminus; C, carboxy terminus. The residue boundaries for each domain are indicated above and are derived from the EF–SAM (2K60.pdb) and SOAR (3TEQ.pdb) structures for cEF, nEF, CC2, and CC3. For STIM1, mutations associated with heritable immunodeficiencies are indicated by a blue arrowhead. The location and sequence of the STIM1L insertion are shown with a green arrowhead. The location and sequence of the long STIM2 ER signal peptide are shown with a green arrowhead. (B) Multiple sequence alignment of human and lower order STIM proteins. *H. sapiens* STIM1 (NCBI, NP_003147.2), *H. sapiens* STIM2 (NCBI, NP_065911.3), *Caenorhabditis elegans* STIM (NCBI, CCD73857.1), and *Drosophila melanogaster* STIM (NCBI, NP_523357.2) sequences were aligned using Clustal Omega (Sievers et al., 2011) with the default settings. The (*) indicates fully conserved residue, (:) strongly similar residues, and (.) weakly similar residue. Conserved residue regions are shaded to correspond with the domain color scheme in A.

the inducible ON/OFF source of Ca^{2+} entry to cells, while STIM2 appears to be more directly involved in basal Ca^{2+} homeostasis (see below).

Human STIM1 and STIM2 each have demonstrated interesting variations in the identity of each respective mature protein. Splice variations in the *STIM1* gene result in a long version of the translated protein (i.e., STIM1L) as well as the shorter, dominant version. STIM1L contains a 106-amino acid insertion in the nonconserved cytosolic region of STIM1, following the conserved CC domains (Fig. 3.1A), and whereas STIM1 is ubiquitously expressed in human tissues, STIM1L is found only in skeletal muscle (Darbellay, Arnaudeau, Bader, Konig, & Bernheim, 2012; Horinouchi et al., 2012). The potency of STIM1L and STIM1 TG-induced activation of SOCE is similar; however, STIM1L has been reported to be critical for fast SOCE activation within myotubes required for repetitive store-dependent Ca^{2+} signals (Darbellay et al., 2012). Interestingly, immunoprecipitation experiments demonstrate that STIM1L binds more abundantly to Orai1 than does STIM1 (Horinouchi et al., 2012). STIM1 encodes a 22-amino acid ER-localization peptide at the N-terminus. STIM2, on the other hand, encodes an additional 87 residues, prior to the homologous ER signal peptide region. It has been suggested that these 87 residues upstream of the STIM1-homologous signal peptide constitutes a much longer signal sequence for STIM2 (Fig. 3.1A), necessary for appropriate ER localization of STIM2 proteins (Graham, Dziadek, & Johnstone, 2011). This 101 residue signal peptide is believed to decrease the ER-localization efficiency of STIM2, resulting in a significant fraction of cytosolic STIM2. Interestingly, it has been suggested that the 101-amino acid signal peptide [i.e., 87 amino acid extended plus 14 amino acid conserved region (Fig. 3.1A and B)] that is cleaved from the ER-inserted STIM2 preprotein may play a role in regulation of gene transcription, independent of SOCE and Orai proteins (Graham et al., 2011).

Human Orai1 is composed of 301 amino acids and has four predicted TM segments (Cai, 2007b) (Fig. 3.2A). Both the N- and C-termini of this PM protein face the cytoplasm, and each plays a role in activation by STIM1 at S/ER–PM junctions (see below). The TM segment 1 (TM1) forms the Ca^{2+} permeation pathway within Orai channels; further, Glu106 in TM1 has been identified as a key residue required for Ca^{2+} ion permeability and selectivity (Prakriya et al., 2006; Yeromin et al., 2006). Glu190 on TM3 may also play a role in ion selectivity (Prakriya et al., 2006). Chemical cross-linking data suggest that residues 88, 95, 102, and 106 are in close apposition to one another, implying that TM1 is centrally located in channel

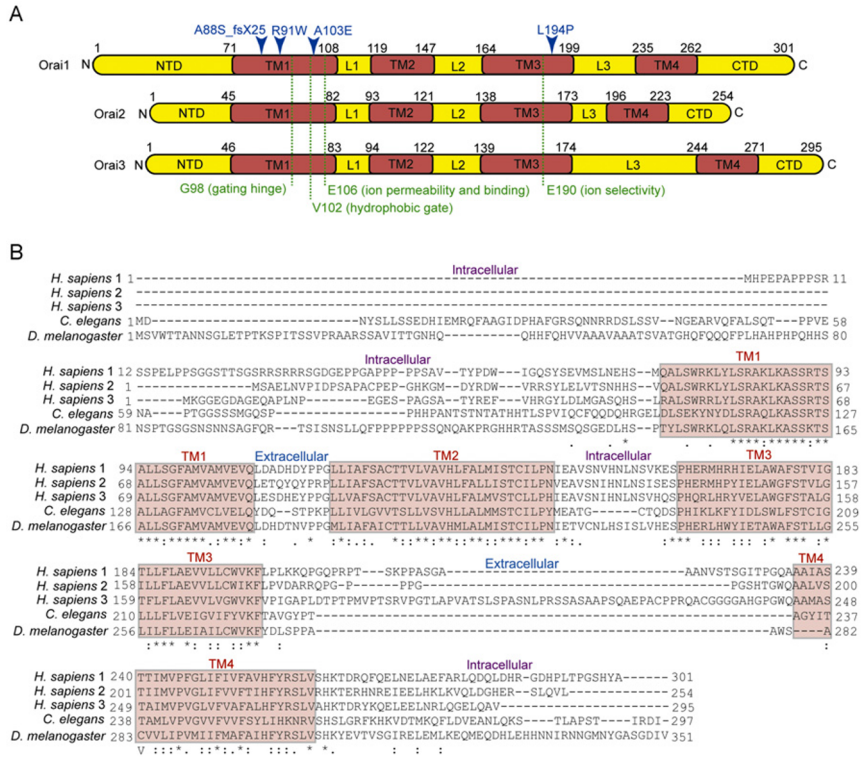

Figure 3.2 Domain architectures and sequence alignments of Orai proteins. (A) The architectures of the three *H. sapiens* homologues, Orai1, Orai2, and Orai3, are shown. NTD, N-terminal domain; TM1, transmembrane region 1; L1, loop 1; TM2, transmembrane region 2; L2, loop2; TM3, transmembrane region 3; L3, loop 3; TM4, transmembrane region 4; CTD, C-terminal domain; N, amino terminus; C, carboxy terminus. The residue boundaries are shown above and are derived from the *D. melanogaster* structure (4HKR.pdb), where each transmembrane region was defined by the uninterrupted helix approximately parallel to the long axis of the pore. For Orai1, mutations associated with heritable immunodeficiencies are indicated with a blue arrowhead. Critical residues for Orai channel function that are conserved among the three homologues are indicated by the green broken lines intersecting the domains. (B) Multiple sequence alignments of human and lower order Orai proteins. *H. sapiens* Orai1 (NCBI, NP_116179.2), *H. sapiens* Orai2 (NCBI, AAH69270.1), *H. Sapiens* Orai3 (NCBI, AAH15555.1), *C. elegans* Orai (NCBI, CCD63979.1), and *D. melanogaster* Orai (NCBI, NP_995881.2) sequences were aligned in Clustal Omega and the output symbols are as described in Fig. 3.1B. The transmembrane regions are shaded to correspond to the boundaries defined in (A), and the regions located intracellularly and extracellularly are indicated above the sequences.

formation (Zhou, Ramachandran, Oh-Hora, Rao, & Hogan, 2010). In an analogous study combining Cys mutagenesis and assessment of thiol reactive agent accessibility, it was also shown that Glu106 is a critical component of the Ca^{2+} permeation pathway which is made of TM1 residues (McNally, Yamashita, Engh, & Prakriya, 2009). Leu95, Gly98, and Val102 are closest to the putative symmetric axis of the channel, and point mutations in Gly98 and Val102 constitutively activate the channel, with substitution type suggesting that Gly98 acts as the gating hinge, while Val102 functions as the gate itself (McNally & Prakriya, 2012; McNally, Somasundaram, Yamashita, & Prakriya, 2012; Zhang et al., 2011).

Humans express three Orai homologues; moreover, these three proteins share a high primary sequence conservation among the residues making up the TM regions, acidic residues involved in ion permeability, residue important for ion selectivity, residue facilitating the gating hinge within TM1, residue forming the hydrophobic gate within the pore, as well as basic residue position associated with SCID (Fig. 3.2B). Recently, a boundary-optimized version of *D. melanogaster* Orai was crystallized as a pore-closed hexamer, confirming that Glu106 (i.e., *D. melanogaster* Glu178) binds Ca^{2+} ions and that Leu95 (i.e., *D. melanogaster* Leu167) and Val102 (i.e., *D. melanogaster* Val174) are important hydrophobic components lining the pore at the axis of symmetry (Hou, Pedi, Diver, & Long, 2012). Human Orai1, Orai2, and Orai3 show a conservation of these important pore residues and are all capable of forming functional CRAC channels with distinct properties when ectopically expressed (Bogeski et al., 2010; DeHaven, Smyth, Boyles, & Putney, 2007; Frischauf et al., 2009; Gwack et al., 2007; Lis et al., 2007). Further, all three homologues are widely expressed in human tissues (Gwack et al., 2007; Schindl et al., 2009); however, Orai1 plays a prevailing role in mediating CRAC entry in immune cells (Feske, Skolnik, & Prakriya, 2012). It should be noted that heterotypic assembly of different Orai proteins and PM-localization of these heteromultimers has been reported (Frischauf et al., 2011; Lis et al., 2007; Mignen, Thompson, & Shuttleworth, 2008; Schindl et al., 2009), suggesting that CRAC channels with distinct functional properties may form in a tissue-dependent manner. That being said, the role of Orai2 and Orai3 in CRAC entry is much less well-understood than Orai1.

Since the discovery of the principal molecular components of CRAC channels, several autosomal recessive mutations in STIM1 and Orai1 have been identified in association with immunodeficiency diseases that present a similar clinical phenotype as SCID (Feske, 2012; Feske et al., 2012).

Inheritable mutations in STIM1 include the Glu128Arg_fsX9 caused by an adenine insertion that results in a frame shift and prematurely terminates STIM1 expression in the SAM domain (i.e., Glu136STOP) (Picard et al., 2009), the 1538-1G>A splice site mutation abrogating full-length *STIM1* mRNA transcription (Byun et al., 2010) and the Arg429Cys which does not affect the full-length expression of STIM1, but exerts a dominant-negative effect on CRAC channel function (Fuchs et al., 2012). Four mutations in Orai1 have been linked with inheritable immunodeficiency diseases. The Ala88Ser_fsX25 mutation terminates Orai1 expression, 25 residues after the open reading frame shift at Ala88 (Feske et al., 2012; Partiseti et al., 1994). The Arg91Trp mutation on TM1 does not interfere with protein expression or Orai1 localization, but eliminates channel function, perhaps through plugging of the pore by the symmetric packing of hydrophobic indole side chains (Feske et al., 2006; Hou et al., 2012; Thompson, Mignen, & Shuttleworth, 2009). Each of the Ala103Glu mutation on TM1 and the Leu194Pro mutation on TM3 result in immunodeficiency; these point substitutions may exert their affects by attenuating protein levels, through destabilization, misfolding, and degradation, for example (Feske et al., 2012; Le Deist et al., 1995). While the aforementioned mutations cause immunodeficiencies, changes in wild-type STIM1 and Orai1 expression levels have been linked with cardiovascular pathophysiologies (reviewed in Zhang & Trebak, 2011) and various cancers (Faouzi et al., 2011, 2013; McAndrew et al., 2011; Motiani, Abdullaev, & Trebak, 2010; Motiani et al., 2013). Additionally, somatic mutations in STIM1, STIM2, Orai1, and Orai2 proteins have also been linked with cancers (Capiod, 2012).

3. STIM1 AND Orai1 IN THE ACTIVATION IN SOCE

The sequence of cellular events leading to SOCE through the STIM and Orai pathway is a multistep process. Within the luminal region, STIMs contain the machinery required to sense Ca^{2+} changes and initiate SOCE. After ER Ca^{2+} store depletion, through the agonist-induced IP_3-mediated pathway, for example, STIM1 self-associates. This oligomerization is prerequisite to the subsequent translocation of STIM1 molecules from a pervasive distribution on the ER to sites which are in close apposition to the PM (i.e., ER–PM junctions) (Liou, Fivaz, Inoue, & Meyer, 2007; Liou et al., 2005; Zhang et al., 2005). At ER–PM junctions, the oligomerized STIM1 recruits Orai1 to the same sites creating a CRAC channel complex (Luik,

Wu, Buchanan, & Lewis, 2006; Varnai, Toth, Toth, Hunyady, & Balla, 2007; Wu, Buchanan, Luik, & Lewis, 2006; Xu et al., 2006). The dynamic redistribution of these proteins is evident in HeLa and HL1 cardiomyocyte cells cooverexpressing monomeric cherry fluorescence protein (mCh)-STIM1 and enhanced green fluorescence protein (eGFP)-Orai1 which show a diffuse mCh and eGFP fluorescence at resting ER Ca^{2+}. After passive ER Ca^{2+} store depletion by external TG addition, mCh-STIM1 forms visible aggregates at ER–PM junctions called puncta; moreover, eGFP-Orai1 also accumulates at these puncta, evident from mCh/eGFP colocalization. Visualization of the cellular fluorescence using total internal reflective fluorescence (TIRF) microscopy reveals that puncta form within ~100 nm of the PM, the distance limit from the plane of the slide in contact with the cell (i.e., the outer PM) for fluorescence excitation by the TIRF technique (Fig. 3.3). These puncta made up of STIM1 and Orai1 proteins form sites of CRAC entry.

Two independent studies demonstrated that an intramolecular transition of the STIM1 cytosolic domains occurs prior to coupling with Orai1 and gating the channel at ER–PM junctions. Using cyan fluorescent protein (CFP) and yellow fluorescent protein (YFP) fused to the N- and C-terminus, respectively, of a cytosolic STIM1 fragment encompassing residues 234–450 [i.e., Orai activating STIM fragment (OASF)] and assessment of the CFP/YFP intramolecular FRET, it was demonstrated that mutations in CC1 (i.e., Leu251Ser) or CC3 (i.e., Leu416Ser/Leu423Ser) could induce an extended conformation (i.e., decreased FRET); moreover, a similar change in FRET was observed upon coupling with and activating Orai1 channels (Muik et al., 2011). Introduction of the same mutations into full-length STIM1 leads to constitutive activation of CRAC entry, independent of ER Ca^{2+} store depletion. In a separate study, FKB12 was fused to a cytosolic fragment of STIM1 encompassing residues 238–462; moreover, it was demonstrated that maximal CRAC activation could only be achieved by this fragment after rapamycin treatment, artificially oligomerizing the molecules with an ER-targeted FRB fragment (Korzeniowski, Manjarres, Varnai, & Balla, 2011). Further, cooverexpression of an FKBP12–STIM1 fusion encompassing residues 238–343 with a spontaneously active FKB12–STIM1 fusion encompassing residues 315–462 that maximally activates Orai1 channels, followed by rapamycin treatment inhibited Orai1 activity (Korzeniowski et al., 2011), suggesting that a region within residues 238–343 is involved in inhibition of the STIM1 conformational transition involved in achieving an Orai1 activation-competent state.

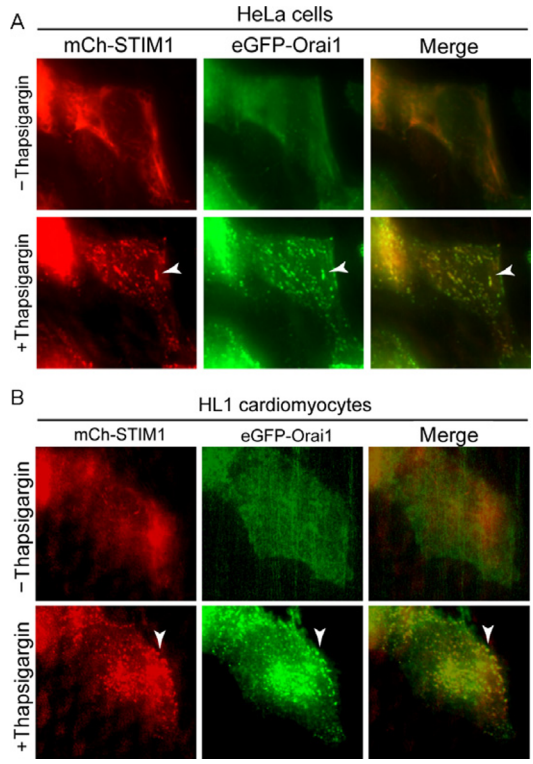

Figure 3.3 Fluorescent microscopy of human STIM1 and Orai1 localization in mammalian cells. (A) HeLa cells cooverexpressing mCh-STIM1 and eGFP-Orai1, visualized using total internal reflective fluorescence (TIRF) microscopy. In the absence of ER Ca^{2+} store depletion, the mCh-STIM1 and eGFP-Orai1 fluorescence are pervasively distributed; upon passive Ca^{2+} store depletion with thapsigargin, the mCh-STIM1 and eGFP-Orai1 form distinct puncta, defined as the clustering of molecules (i.e., and fluorescence) at ER–PM junctions (white arrowheads). When the images are merged, the eGFP-Orai1 and mCh-STIM1 exhibit a coclustering (yellow fluorescence). The TIRF mode limits fluorescence excitation within ~100 nm of the PM. (B) HL1 cardiomyocytes cooverexpressing mCh-STIM1 and eGFP-Orai1, visualized using TIRF. Upon passive sarcoplasmic reticulum (SR) Ca^{2+} store depletion using thapsigargin, a similar redistribution of mCh-STIM1 and eGFP-Orai1 is observed in these electrically excitable cells as for HeLa cells. In (A) and (B), cells were bathed in HBSS plus 1.5 mM $CaCl_2$. Images were taken at ambient temperature, before and 5 min post thapsigargin addition (2 μM external).

Deletion of the C-terminal tail of STIM1 prevents translocation to ER–PM junctions after S/ER Ca^{2+} store depletion (Baba et al., 2006; Park et al., 2009). This effect has been attributed to the Lys-rich region of STIM1. Remarkably, cooverexpression of truncated STIM1 with Orai1 rescues

translocation and activation of CRAC channels (Muik et al., 2009; Park et al., 2009; Yuan et al., 2009). STIM proteins in lower order organisms such as *D. melanogaster* do not contain this polybasic region (Cai, 2007a), suggesting that the STIM poly-Lys-mediated mechanism of translocation and the STIM CC-mediated coupling and recruitment of Orai1 (see below), where the CC region is highly conserved among all phylogeny (Fig. 3.1B), are two separable processes. Several cell biology studies suggest that the STIM1 poly-Lys region interacts with membrane PIP_2, as membrane depleting and supplementing agents inhibit and enhance translocation, respectively (Calloway et al., 2011; Korzeniowski et al., 2009; Walsh et al., 2010). These observations reinforce the complexity of Ca^{2+} signaling, as receptor-mediated activation of SOCE involves the conversion of PIP_2 to IP_3 and diacylglycerol by phospholipases, yet PIP_2 depletion is inhibitory to the entire process.

4. HUMAN STIM1 AND STIM2 EF–SAM BIOPHYSICAL FEATURES

Mobilization of the molecular components involved in SOCE is initiated in the ER lumen after Ca^{2+} store depletion. The EF-hand together with SAM domain of STIMs (i.e., EF–SAM) is highly conserved from lower to higher order eukaryotes. *In vitro* studies show that EF–SAM can be recombinantly expressed and isolated with high purity from *Escherichia coli* (Stathopulos, Li, Plevin, Ames, & Ikura, 2006). Remarkably, the two domains fold cooperatively indicative of the mutual dependency of the two domains on the conformational stability of the region. The isolated EF–SAM region of STIM1 exhibits drastic conformational differences in the presence and absence of Ca^{2+} (Stathopulos et al., 2006). In the presence of Ca^{2+}, STIM1 EF–SAM demonstrates high α-helicity, in a monodisperse monomeric conformation. In the absence of Ca^{2+}, STIM1 EF–SAM loses a considerable amount of α-helicity and forms a polydisperse solution of dimers and oligomers (Stathopulos, Zheng, Li, Plevin, & Ikura, 2008). The well-folded and monodisperse character of the Ca^{2+}-loaded state compared to the partially folded polydisperse and oligomerized character of the Ca^{2+}-depleted state is clearly evident in the ^{1}H–^{15}N heteronuclear quantum single coherence (HSQC) nuclear magnetic resonance (NMR) spectra where the Ca^{2+}-loaded protein spectrum is well-dispersed and each amide $^{1}H(N)$ resonance is resolved versus the Ca^{2+}-depleted protein spectrum which exhibits the $^{1}H(N)$ resonances clustered in the unfolded ^{1}H chemical

shift region (i.e., ~7.5–8.5 ppm) and many resonances broadened beyond detection (Stathopulos et al., 2006). The broadening observed in the Ca^{2+}-depleted NMR spectra is due to conformational exchange of the unfolded regions of EF–SAM, the polydisperse nature of the oligomers (i.e., dimers and high-order oligomers) diluting the resonances in multiple quaternary structures and the decreased tumbling time of the larger order oligomers which undergo fast relaxation of magnetization.

In nature, EF-hand motifs are predominantly found in pairs, promoting backbone hydrogen bonding between the loop regions of these helix-loop-helix motifs and stabilizing the Ca^{2+}-binding sites and the entire EF-hand domain (reviewed in Gifford, Walsh, & Vogel, 2007; Ikura & Ames, 2006). STIM proteins exhibit only a single primary sequence-identifiable EF-hand motif. Assessment of STIM1 EF–SAM Ca^{2+} binding using a $^{45}Ca^{2+}$ equilibrium ultrafiltration procedure, as well as by monitoring changes in secondary structure and intrinsic Trp fluorescence of EF–SAM as a function of Ca^{2+} concentration revealed that the EF–SAM domain binds a single Ca^{2+} atom with relatively low affinity (i.e., equilibrium dissociation constant, $K_d \sim 200–600\ \mu M$) (Huang et al., 2009; Stathopulos et al., 2006; Zheng et al., 2011). Nevertheless, the experimentally derived *in vitro* Ca^{2+} affinity of STIM1 EF–SAM is in the range of Ca^{2+} levels documented for the ER lumen (Feske, 2007), suggesting that the Ca^{2+}-binding property of EF–SAM is sensitive to fluctuations in ER Ca^{2+} associated with SOCE.

Human STIM2 EF–SAM has been successfully expressed and purified recombinantly from *E. coli* (Zheng, Stathopulos, Li, & Ikura, 2008). In the presence of Ca^{2+}, STIM2 EF–SAM is well-folded and contains high α-helicity, as per STIM1 EF–SAM. Unlike STIM1 EF–SAM which markedly loses α-helicity in the absence of Ca^{2+}, STIM2 EF–SAM retains much of the α-helicity observed in the Ca^{2+}-loaded state, after Ca^{2+} depletion. At 4 °C, the far-UV circular dichroism (CD) spectrum of STIM2 EF–SAM shows two intense minima at 208 and 225 nm, indicative of high α-helicity; moreover, after Ca^{2+} depletion, the two minima are retained in STIM2 EF–SAM with only a marginal decrease in negative ellipticity (Zheng et al., 2008). In the case of STIM1, the Ca^{2+}-depleted far-UV-CD spectrum markedly loses the negative ellipticity associated with both the 208 and 225 nm bands and the 208 nm band shifts to lower wavelength, suggesting a partial unfolding. A loss of regular secondary structure is usually associated with a decrease in conformational stability; moreover, thermal melts are often employed as a straightforward assessment of protein stability, where a

spectroscopic signal reporting on the structure of a protein is monitored as a function of temperature. STIM1 and STIM2 EF–SAM thermal melts monitored by far-UV-CD at 225 nm exhibit apparent midpoints of temperature denaturation (T_m) of ~45 and 50 °C, respectively, in the Ca^{2+}-loaded state. In the Ca^{2+}-depleted state, STIM1 exhibits a T_m of ~21 while STIM2 EF–SAM is ~36 °C (Zheng et al., 2008, 2011). The differences in T_m in the apo versus holo state (i.e., ΔT_m) is ~−14 °C for STIM2 EF–SAM compared to ~−24 °C for STIM1 EF–SAM. These stability parameters are consistent with the much lesser affect of Ca^{2+} depletion on the far-UV-CD spectrum of STIM2 EF–SAM compared to STIM1 EF–SAM and suggest that STIM1 EF–SAM more readily undergoes a structural transformation in response to Ca^{2+} depletion than STIM2 EF–SAM.

Size exclusion chromatography with in-line multiangle light scattering (SEC-MALS) has been an important tool used to assess the oligomerization state of STIM proteins. At 4 °C, STIM1 EF–SAM transitions from a monomer to a dimer and higher order oligomers after Ca^{2+} depletion (Stathopulos et al., 2008). On the other hand, STIM2 EF–SAM resists the oligomerization observed for STIM1 EF–SAM, maintaining a monomeric conformation at stabilizing low temperatures upon Ca^{2+} depletion. At 25 °C, STIM2 EF–SAM readily aggregates after Ca^{2+} depletion demonstrated by the void volume elution in SEC-MALS experiments and severely broadened ^{1}H–^{15}N-HSQC spectra, suggesting that this region of STIM2 possesses an innate ability to oligomerize in a Ca^{2+}-depletion-dependent manner (Zheng et al., 2008), as per STIM1; however, STIM2 EF–SAM demonstrates a markedly reduced propensity for oligomerization compared to the STIM1 counterpart (Stathopulos, Zheng, & Ikura, 2009). These distinctions in oligomerization propensity are related to the aforementioned structural stability differences. The importance of EF–SAM oligomerization to full-length physiological function of STIM1 was demonstrated in an elegant study where the EF–SAM region of STIM1 was replaced by FKBP12 and FK506 domains, and oligomerization of these domains was induced chemically by rapamycin which can freely diffuse through cell membranes (Luik, Wang, Prakriya, Wu, & Lewis, 2008). This FKBP12–STIM1 chimera showed no ER Ca^{2+} sensitivity; however, rapamycin treatment, which artificially oligomerized the luminal region of the chimera, resulted in SOCE activation. Additionally, FRET data demonstrated that STIM1 proteins truncated after the TM region display little intermolecular FRET at resting ER Ca^{2+}; on the other hand, ER Ca^{2+} depletion results in a high intermolecular FRET indicative of the self-association of this region in a

Ca^{2+}-depletion-dependent manner (Covington, Wu, & Lewis, 2010). Overall, these data suggest that EF–SAM oligomerization is an important initiation mechanism for STIM1 activation and *in vitro* assessment of the self-association propensity of this region can be used as a readout of the propensity for SOCE initiation.

Kinetics of EF–SAM oligomerization has been evaluated directly by changes in light scattering intensity as a function of time and indirectly by monitoring changes in secondary structure as oligomerization is coupled to partial unfolding of the EF–SAM region. Using these biophysical probes, it has been demonstrated that Ca^{2+}-depleted STIM2 EF–SAM undergoes a much slower transformation to an oligomerized state compared to STIM1 EF–SAM. Consistent with the greater propensity and faster kinetics of oligomerization, STIM1 EF–SAM exhibits greater than threefold faster urea-induced unfolding rates compared to STIM2 EF–SAM (Stathopulos et al., 2009).

Human STIM2 has been implicated in the regulation of resting cytosolic and ER luminal Ca^{2+} levels (Brandman, Liou, Park, & Meyer, 2007). This role in basal Ca^{2+} homeostasis has been attributed to the fact that STIM2 activates Orai1 at basal ER Ca^{2+}, and is more sensitive to small changes in ER Ca^{2+} levels than STIM1. Biophysically, STIM2 EF–SAM has increased stability and decreased propensity for oligomerization than STIM1; however, the Ca^{2+} affinity of STIM2 EF–SAM, assessed by changes in secondary structure as a function of Ca^{2+}, is lower than that assessed for STIM1 (i.e., $K_d \sim 600$–800 μM) (Zheng et al., 2011). Hence, a larger fraction of STIM2 molecules is in the Ca^{2+}-depleted state at basal ER Ca^{2+} compared to STIM1. Nevertheless, a fraction of STIM2 can also be activated after receptor-mediated ER Ca^{2+} store depletion, suggesting that STIM2 also plays a role in SOCE.

5. HUMAN STIM1 EF–SAM STRUCTURE

The modular architecture of STIM proteins has facilitated a fragmentary approach to elucidating atomic resolution structural information on these proteins. The first atomic resolution structure solved on any component of the CRAC complex was Ca^{2+}-loaded STIM1 EF–SAM (Stathopulos et al., 2008). This ER lumen-residing region of STIM1 encompassing residues 58–201 folds into a primarily α-helical protein consisting of 10 helices (Fig. 3.4A). Remarkably, the STIM1 EF–SAM structure revealed that despite only a single primary sequence-identifiable EF-hand, a second EF-hand exists,

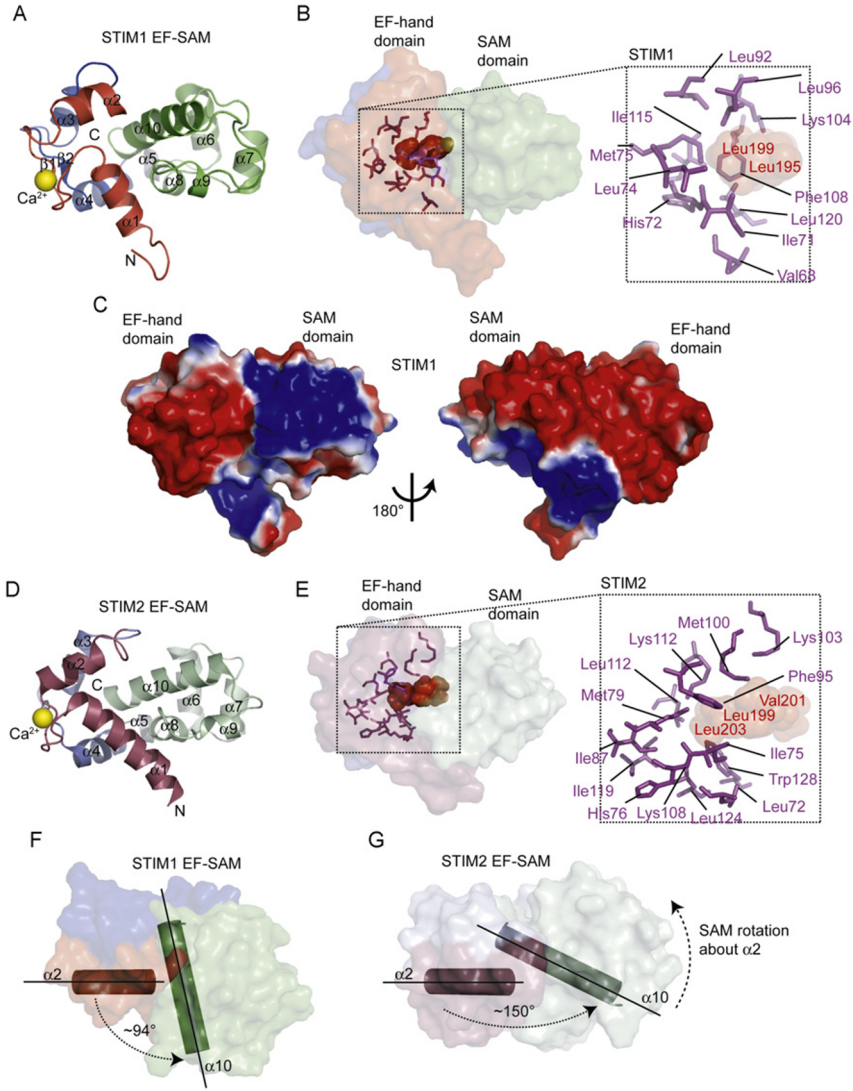

Figure 3.4 Structural features and comparison of human STIM1 and STIM2 luminal domains. (A) Structure of human Ca^{2+}-loaded STIM1 EF–SAM (2K60.pdb). The 10 α-helices and 2 β-strands making up the compact EF–SAM structure are labeled. N, amino terminus; C, carboxy terminus; Ca^{2+} (yellow sphere), calcium ion. Motif coloring corresponds to Fig. 3.1A, with α5 shown in gray. (B) STIM1 EF-hand:SAM domain intramolecular interaction, stabilizing the monomeric conformation. The surface representation is shaded as in (A). The principal side chains forming the EF-hand hydrophobic pocket are shown (sticks). The SAM hydrophobic protrusion residues are illustrated (spacefill). The zoomed view of the intimate hydrophobic contacts in the interface

(Continued)

forming an EF-hand pair through backbone hydrogen bonding of the loops. The canonical EF-hand motif is made up of α1-β1-α2 secondary structure components, while the α3-β2-α4 components make up the noncanonical EF-hand. The carbonyl oxygen atoms [i.e., C(O)] of Val83 and Ile115 in β1 and β2, respectively, and the amide protons [i.e., N(H)] of Val83 and Ile115 form two hydrogen bonds, creating a short β-sheet. A short α-helix links the EF-hand domain to the SAM domain in sequence space.

Interestingly, the STIM1 EF-hand pair is most structurally similar to the C-terminal EF-hand pair of Ca^{2+}-loaded calmodulin (CaM), even though the noncanonical EF-hand of STIM1 does not bind Ca^{2+} (Stathopulos et al., 2008). In Ca^{2+}-loaded C-CaM, the interhelix angles are 81.4° and 107.7°, each adopting an "open" conformation. In STIM1 EF–SAM, the canonical and noncanonical EF-hand interhelix angles are 80.0° and 96.7°, respectively, also in an "open" conformation. "Open" EF-hands expose hydrophobic side chains for interaction with binding partners (Gifford et al., 2007; Ikura & Ames, 2006). The STIM1 SAM domain folds into a 5-helix bundle (i.e., α6–α10) and is structurally similar to many other SAM domains, the most homologous being the EphB2 receptor. The EF-hand and SAM domains are not structurally independent from one

Figure 3.4—Cont'd (broken black boxes) is shown at right. The individual EF-hand residues (purple sticks) and the SAM residues (red spacefill) are labeled. (C) Electrostatic surface of Ca^{2+}-loaded STIM1 EF–SAM. The electrostatic surface shown with a +1 (blue) to −1 (red) *kT/e* gradient was calculated using the APBS tools (Baker, Sept, Joseph, Holst, & McCammon, 2001) in PyMOL (The PyMOL Molecular Graphics System, Schrödinger, LLC) with data generated from the PDB2PQR server (Dolinsky et al., 2007). (D) Structure of human Ca^{2+}-loaded STIM2 EF–SAM (2L5Y.pdb). The 10 α-helices making up the compact EF–SAM structure are labeled. The two EF-hands exhibit hydrogen bonding between loops, although no β-sheet was identifiable. Motif coloring is as per (A), with different shades of red (raspberry), blue (slate), and green (pale green) to be distinguishable from STIM1. N, amino terminus; C, carboxy terminus; Ca^{2+} (yellow sphere), calcium ion. (E) STIM2 EF-hand:SAM domain intramolecular interaction. The surface representation is shaded as in (C). The principal side chains forming the EF-hand hydrophobic pocket are shown (sticks). The SAM hydrophobic protrusion residues are illustrated (spacefill). The zoomed view of the intimate hydrophobic contacts in the interface (broken black boxes) is shown at right. The individual EF-hand residues (purple sticks) and the SAM residues (red spacefill) are labeled. (F) Orientation of the STIM1 SAM relative to the EF-hand domain. The α2 (i.e., within the cEF) and α10 (i.e., within the SAM) interhelix angles are semiperpendicular (i.e., ∼94°) in Ca^{2+}-loaded STIM1 EF–SAM. (G) Orientation of the STIM2 SAM relative to the EF-hand domain. The α2 and α10 interhelix angles are semiparallel (i.e., ∼150°) in Ca^{2+}-loaded STIM2 EF–SAM. In (F) and (G), the view is 90° into the page relative to (B) and (E), respectively.

another; rather, they intimately interact through a robust interface (Fig. 3.4B). Residues from both "open" EF-hands contribute to the creation of an extensive hydrophobic pocket, reminiscent of the inside palm of a hand. Val68, Ile71, His72, Leu74, Met75, and Leu92 from the canonical EF-hand and Leu96, Lys104, Phe108, Ile115, and Leu120 from the non-canonical EF-hand form the cleft. The SAM domain packs tightly into the EF-hand hydrophobic pocket with residues on the α10 helix forming a hydrophobic protrusion. The most projected residues on the SAM domain include Leu195 and Leu199 which behave as hydrophobic anchors for the EF-hand pocket. The SAM domain fits into the EF-hand cleft like a fist into the palm of a hand. Together, both the EF-hand domain and the SAM domain of STIM1 fold into a compact globular shape. The electrostatic surface of Ca^{2+}-loaded STIM1 EF–SAM is primarily acidic, promoting aberrant migration on SDS-PAGE gels. However, a small positive region exists on the surface of the SAM domain (Fig. 3.4C). The positive region may serve to electrostatically guide Ca^{2+} ions (i.e., via repulsion) to the more negative EF-hand region of EF–SAM; additionally, this electropositive patch may promote binding to other ER proteins or membrane lipids as reported for other SAM domains (Kim & Bowie, 2003; Koveal et al., 2012) and is consistent with the close apposition of EF–SAM to the inner leaflet of the ER membrane.

Through mutational analyses, it has been demonstrated that the intramolecular EF-hand:SAM domain interaction is a structural feature that plays a critical role in the regulation of STIM1 oligomerization. Mutations within the canonical Ca^{2+}-binding loop of EF–SAM which abrogate Ca^{2+} coordination result in the oligomerization of STIM1 and the formation of puncta, independent of ER Ca^{2+} store depletion (Liou et al., 2005; Luik et al., 2006; Zhang et al., 2005). Remarkably, mutations which disrupt the EF-hand:SAM domain interface also induce oligomerization, puncta formation, and SOCE activation, but keep the native Ca^{2+}-binding properties of EF–SAM completely intact (Stathopulos et al., 2008). Furthermore, biophysical analyses on EF–SAM demonstrate a partial unfolding upon Ca^{2+} depletion is coupled with a high propensity for oligomerization. Mutations which perturb the EF-hand:SAM domain interface (i.e., Leu195Arg—SAM anchor disruption and Phe108Asp/Gly110Asp—EF-hand cleft disruption) also partially unfold EF–SAM and promote oligomerization of this domain. Hence, the loss in stability due to disruption of the EF-hand:SAM domain interface and the subsequent coupled oligomerization is a key mechanistic step in initiating SOCE activation. In the native protein, it is tempting to

speculate that a closure of the EF-hand renders the hydrophobic cleft residues inaccessible to the SAM anchor residues, destabilizing both domains. The large heterogeneity in oligomerized Ca^{2+}-depleted EF–SAM prevents the extraction of high-resolution structural information. Nevertheless, negative-stain transmission electron microscopy has demonstrated that oligomerized EF–SAM form amorphous aggregates rather than the ordered polymeric filaments observed previously for other SAM domains (e.g., TEL, Yan, Scm, and polyhomeotic) (Stathopulos et al., 2008). Taken together, the live cell data demonstrating that oligomerization of the luminal STIM1 domains initiates SOCE, the structural data elucidating the robust and non-mutually exclusive structure of the EF-hand and SAM domains, the biophysical experiments revealing the Ca^{2+}-depletion-induced loss in stability and increased propensity for oligomerization, and the estimated Ca^{2+}-binding affinity of EF–SAM in the range of physiological ER Ca^{2+} levels, suggest that EF–SAM domains within STIM molecules sense Ca^{2+} depletion in the ER lumen through a destabilization-coupled oligomerization, a structural change which initiates further downstream alterations to the cytosolic domains that is fundamental to the activation of SOCE.

6. HUMAN STIM2 EF–SAM STRUCTURE

Structurally, human STIM2 EF–SAM is highly homologous to STIM1, as the two human homologues share 85% sequence identity through the EF–SAM region (Zheng et al., 2011). Despite this high sequence similarity, STIM2 EF–SAM has distinct biophysical characteristics and the full-length molecule exhibits a unique role in basal Ca^{2+} homeostasis (see above). In the presence of Ca^{2+}, STIM2 EF–SAM folds into a 10-helix globular structure (Fig. 3.4D). A noncanonical EF-hand is located adjacent to the noncanonical EF-hand, and a short linker helix links the EF-hand pair to the 5-helix bundle SAM domain. The loops of the EF-hand motifs are mutually stabilized through hydrogen bonding [i.e., Ile119 C(O):Ile 87 N(H)]. A hydrophobic cleft is formed by the two EF-hands; however, the STIM2 EF-hand hydrophobic pocket is more extensively concentrated with nonpolar side chains than STIM1 (Zheng et al., 2011). The canonical STIM2 EF-hand positions Leu72, Ile75, His76, Met79, Ile87, and Phe95 side chains in the cleft, while the noncanonical EF-hand contributes Met100, Lys103, Lys108, Leu112, Ile119, Leu124, and Trp128 side chains to the cleft

(Fig. 3.4E). In STIM2 EF–SAM, the Trp128 (i.e., Trp124 in STIM1) and Lys103 (i.e., His99 in STIM1) are located outside of the cleft. The STIM2 SAM domain has Leu199 and Leu203 side chains at the distal end of the α10 helix which are oriented into the EF-hand hydrophobic pocket; moreover, the STIM2 α10 helix has an additional nonconserved Val201 (i.e., Thr197 in STIM1) which contributes to the stability of the STIM2 EF-hand:SAM domain interaction.

The more extensive hydrophobic cleft found in STIM2 EF–SAM allows the SAM domain to rotate away from the canonical EF-hand motif. This rotation is exemplified in the α2–α10 interhelix angle which is ∼150° in STIM2 EF–SAM (i.e., semiparallel) compared to ∼94° in STIM1 EF–SAM (i.e., semiperpendicular) (Fig. 3.4F and G), and allows Asp200 of the STIM2 α10 helix to position itself in close apposition to the oppositely charged Lys108 of the noncanonical EF-hand (Zheng et al., 2011). The increased stability of Ca^{2+}-loaded STIM2 EF–SAM is in part due to the enhanced EF-hand:SAM domain interactions. Nevertheless, it is important to note that the STIM2 SAM domain buries 12 nonpolar residues in the SAM core (i.e., Leu142, Leu145, Val149, Phe158, Val163, Leu168, Met179, Ile180, Leu183, His190, Lys193, and Leu194) with greater than 95% solvent inaccessibility compared to only nine residues in the STIM1 SAM domain (i.e., Val137, Leu141, Val145, Leu159, Leu167, Met174, His186, Leu190, and Ala194) (Zheng et al., 2011). The hydrophobic rearrangement for the STIM2 SAM domain is due to the presence of Ile180, which is not conserved in STIM1 (i.e., Gly176 in STIM1); further, the STIM2 Phe158 and Lys193 are included in the STIM2 SAM core, whereas the aligned Phe154 and Lys189 in STIM1 are excluded.

Despite these structural differences, the individual motifs within EF–SAM are remarkably interchangeable, and this type of chimeric approach elegantly reveals information about the bases for the functional differences between human STIM1 and STIM2. After defining the canonical EF-hand, noncanonical EF-hand and SAM structural motifs as the building blocks of the EF–SAM domain, every combination of STIM1–STIM2 EF–SAM chimera was engineered, and while pure protein was unattainable from one combination (i.e., STIM*2* canonical EF-hand-STIM*2* noncanonical EF-hand-STIM*1* SAM domain, named ES-*221*), highly pure recombinant EF–SAM protein was attainable from all other combinations. Using this chimeric approach, both a "super-stable" and "super-unstable" EF–SAM were engineered (Zheng et al., 2011). The "super-stable" EF–SAM was made up of the STIM*1*

canonical EF-hand, STIM*2* noncanonical EF-hand, and STIM*2* SAM domain (i.e., ES-122); further, this composition is congruent with the higher Ca^{2+}-binding affinity of the STIM1 canonical EF-hand, combined with the increased hydrophobicity of the EF-hand cleft afforded by additional STIM2 noncanonical residues Lys103 and Trp128, additional STIM2 SAM domain hydrophobic anchor and the increased core hydrophobicity of the STIM2 SAM domain. As expected, the "super-unstable" EF–SAM chimera (i.e., ES-211) combined the low Ca^{2+}-binding affinity of the STIM*2* canonical EF-hand with the reduced hydrophobicity of the STIM*1* noncanonical EF-hand and the reduced stability of the STIM*1* SAM domain. *In vitro*, the "super-stable" ES-122 exhibited significantly enhanced thermal stabilities compared to wild-type STIM1 or STIM2 EF–SAM in the Ca^{2+}-loaded and Ca^{2+}-depleted states. In contrast, the "super-unstable" ES-211 EF–SAM showed attenuated thermal stabilities in both the Ca^{2+}-loaded and the Ca^{2+}-depleted states compared to wild-type STIM1 or STIM2 EF–SAM. More importantly, consistent with the notion that EF–SAM stability mediates the initiation of SOCE through STIMs, live cells expressing the "super-stable" ES-122 EF–SAM in place of the wild-type EF–SAM in the full-length STIM1 protein demonstrated significantly decreased maximal inward rectifying currents and increased times to maximal activation after ER Ca^{2+} store depletion. On the other hand, cells expressing STIM1 harboring the "super-unstable" ES-211 EF–SAM in place of the wild-type EF–SAM exhibited spontaneous and maximally active CRAC channels in the absence of ER Ca^{2+} store depletion (Zheng et al., 2011).

Overall, the high-resolution structural data elucidated for STIM1 and STIM2 EF–SAM combined with the *in vitro* biophysical and live cell functional analyses have revealed three critical aspects in SOCE regulation. First, the EF–SAM region of STIM proteins is metastable so that Ca^{2+} binding or release can induce marked structural changes in association with a gain or loss in stability, respectively; second, the EF-hand:SAM domain interaction is a key mediator of conformational stability, where Ca^{2+} depletion disrupts the interaction and induces a partial unfolding-coupled oligomerization; third, the differences in STIM1 and STIM2 function can be partly attributed to a divergent balance between EF-hand Ca^{2+}-binding affinity and SAM domain stability, where STIM1 binds Ca^{2+} with higher affinity than STIM2, but STIM2 has a more stable SAM domain compared to STIM1. STIM1 is an effective ON/OFF regulator of SOCE as the higher Ca^{2+} affinity renders it less susceptible to marginal changes in ER Ca^{2+}; however, upon reaching an ER Ca^{2+} depletion threshold, the lower SAM stability

and less robust EF-hand:SAM interface facilitate increased kinetics of oligomerization compared to STIM2. On the other hand, STIM2 plays a role in basal Ca^{2+} homeostasis as the lower Ca^{2+} affinity confers an increased sensitivity to small decreases in ER Ca^{2+} compared to STIM1; however, the increased stability of the Ca^{2+}-depleted STIM2 EF–SAM prevents hyperactivation of CRAC channels through decreased propensity for oligomerization and attenuated kinetics of this self-association.

7. HUMAN STIM1 AND STIM2 CYTOSOLIC DOMAINS

While the STIM luminal domains regulate the initiation of SOCE, the cytosolic domains play a crucial role in further STIM oligomerization, stabilization of the oligomers, targeting oligomerized STIM molecules to ER–PM junctions, coupling to and recruitment of the Orai subunits, gating of the CRAC channel pore, and channel inactivation (Covington et al., 2010; Derler et al., 2009; Muik et al., 2009; Park et al., 2009). Several independent studies showed that the cytosolic domains within STIM1, conserved from lower to higher eukaryotes, can constitutively activate Orai1 channels in the absence of the luminal domains and without anchoring to the ER membrane. The OASF, encompassing residues 233–450, or 233–474 in a longer version, was shown to induce Ca^{2+}-selective inward rectifying Orai1 currents, independent of ER luminal Ca^{2+}, and colocalize with Orai1 (Muik et al., 2009). The minimal boundaries within OASF to couple with Orai1 and spontaneously induce maximal inward rectifying currents were later defined by the CRAC activating domain (CAD; residues 342–448) (Park et al., 2009), the STIM-Orai activating region (SOAR; residues 344–442) (Yuan et al., 2009), and ccb9 (i.e., residues 339–446) (Kawasaki, Lange, & Feske, 2009). The putative CC3 region within OASF and CAD has been shown to be important in homotypic oligomerization of these cytosolic domains (Covington et al., 2010; Muik et al., 2009). In fact, the oligomers formed by EF–SAM upon ER Ca^{2+} depletion are more susceptible to dissociation at high salt concentrations than the oligomers, subsequently formed by the CAD region. In particular, STIM1 residues 420–450 augment STIM1 homomerization concomitant with CRAC channel activation (Muik et al., 2009), and residues 392–448 stabilize higher order STIM1 oligomers against salt-induced dissociation (Covington et al., 2010).

In the absence of Orai1 cooverexpression, human OASF, CAD, and SOAR demonstrate a pervasive distribution within the cytosol; however, in the presence of Orai1 cooverexpression, these constructs colocalize with

Orai1 into aggregates near the PM (Muik et al., 2009; Park et al., 2009; Yuan et al., 2009). This behavior is in contrast to STIM1 constructs which retain the polybasic region at the distal C-terminal region and are capable of translocating into puncta without Orai1 cooverexpression (see above).

Recently, an X-ray crystallography structure of human SOAR, mutated to stabilize a dimeric state, has revealed information on the atomic organization of this region capable of maximally activating CRAC channels (Yang, Jin, Cai, Li, & Shen, 2012). A Leu374Met/Val419Ala/Cys437Thr triple mutant exhibited three different dimer interfaces from four identical molecules in the asymmetric unit. Based on buried surface area, a symmetric dimer was deemed the physiological relevant state, forming a V-shape. Within each subunit, extensive intramolecular CC2:CC3 interactions are observable (Fig. 3.5A). Interestingly, a *Caenorhabditis elegans* structure of cytosolic STIM residues 212–410, corresponding to human residues 233–465 was also solved by the same group, substantiating the dimer interface (Yang et al., 2012). Although most of CC1 shows no electron density, *C. elegans* residues 257–279, corresponding to human 307–337, form a helix designated the "inhibitory" helix. This "inhibitory" helix makes contacts with the SOAR region, and it has been suggested that this interaction keeps STIM in a quiescent state, as deletion of the homologous region in human STIM1 results in constitutive CRAC channel activation, independent of ER luminal Ca^{2+} (Yang et al., 2012). It should be noted that human residues 310–317 are not conserved in the *C. elegans* homologue, and thus, some fundamental differences between the worm and human structures must exist in this region. Consistent with these differences, *C. elegans* STIM has been reported to be distributed into puncta even at basal Ca^{2+}, and *C. elegans* C-terminal chimeras (i.e., human 234–685 cloned into the equivalent *C. elegans* region) partially convert the chimera localization to a diffuse, human-like distribution (Gao et al., 2009; Lorin-Nebel, Xing, Yan, & Strange, 2007; Yan et al., 2006).

8. STIM COUPLING TO Orai

Orai proteins have an N-terminal region, C-terminal region, and an intracellular loop oriented in the cytosol (Fig. 3.2B). A yeast-two-hybrid approach was employed to show that human STIM1 CAD interacts with the N- and C-termini of Orai1, but not the sole intracellular Orai1 loop (Park et al., 2009). Further, Orai1 truncation studies demonstrated that removal of Orai1 residues 1–91 (i.e., cytosolic N-terminus) or 257–301 (i.e., cytosolic C-terminus) abolished CRAC current measurements (Park

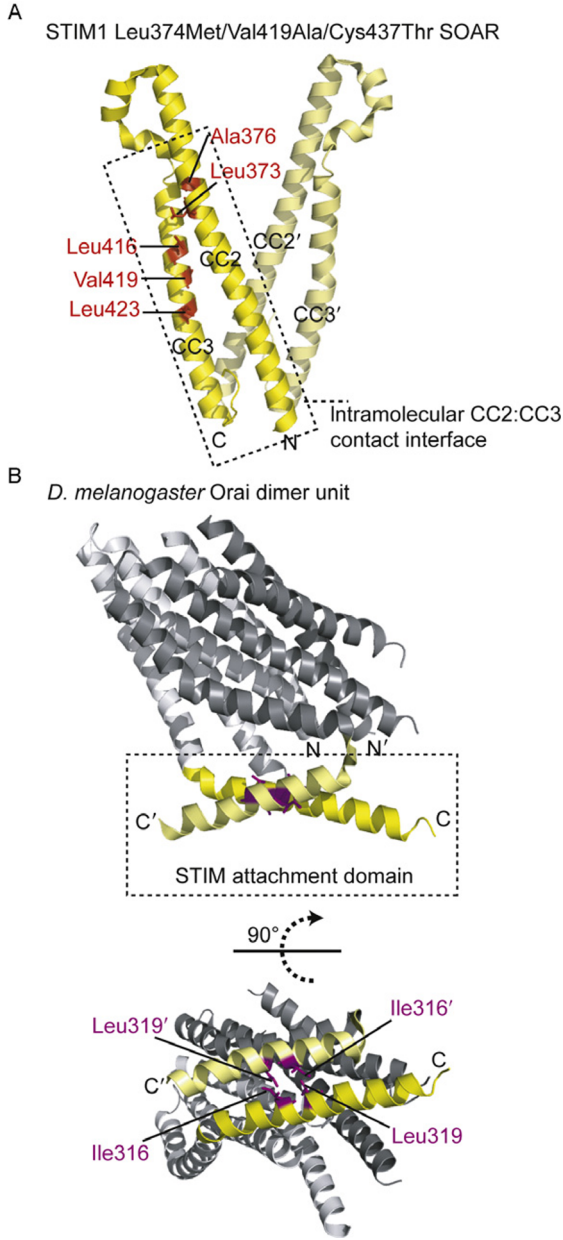

Figure 3.5 Human SOAR and *D. melanogaster* Orai structures. (A) Dimer structure of human Leu374Met/Val419Ala/Cys437Thr SOAR (3TEQ.pdb). The dimer illustrated is one of three different dimer units in the asymmetric cell, formed by identical monomer conformations. Each monomer is a different shade of yellow. Extensive CC2:CC3 intramolecular contacts are observed (broken black box) keeping CC2 and CC3 in an

(Continued)

et al., 2009; Yuan et al., 2009). Interestingly, while removal of the N-terminal region of Orai1 eliminated CRAC channel currents, Orai1 retained the ability to colocalize and cluster with CAD (Park et al., 2009). Further, within the N-terminal region of Orai1, residues ~66–91 bind tighter than the full N-terminal domain (i.e., residues 1–91), and Orai1 is still capable of channel activity after deletion of residues 1–70 (Park et al., 2009). Overall, the C-terminal domain of Orai1 appears to bind tighter to STIM1 than the N-terminal domain, but both are requisite for CRAC channel activation (Frischauf et al., 2009; Muik et al., 2008; Muik, Schindl, Fahrner, & Romanin, 2012; Park et al., 2009; Yuan et al., 2009; Zhou, Meraner, et al., 2010).

Human STIM1 CAD (i.e., residues 342–448) exhibits ~76% primary sequence identity and ~91% similarity with STIM2 CAD (Fig. 3.1B). The high level of amino acid conservation within this minimal CRAC activating region implies that the mode of coupling with and activation of Orai1 is principally similar between the two STIM homologues. The small variations in the amino acid sequence of CAD could result in subtle structural differences that contribute to functional distinctions between STIM1 and STIM2, as observed with the EF–SAM domains; however, less well-conserved regions between STIM1 and STIM2 within the ER luminal domains (Zhou et al., 2009) and the cytosolic regions likely play a more dominant role in the differential modulation of Orai1 channel activity. The human Orai1 N-terminal region (i.e., residues 66–91) which interacts with CAD and is required for channel gating is highly conserved in human Orai2 and Orai3 (i.e., ~89% and 77% sequence identity, respectively) (Fig. 3.2B). Nevertheless, the three human homologues share little sequence similarity through the remaining intracellular N-terminal residues. The C-terminal domain of Orai1 (i.e., residues 257–301) which more strongly binds to CAD exhibits ~36% and 44% sequence identity with human Orai2 and Orai3, respectively (Fig. 3.2B). The

Figure 3.5—Cont'd antiparallel orientation. Mutated residues positions which cause an intramolecular conformational extension within the STIM1 cytosolic domains (i.e., minimum of 15% decrease in CFP-OASF-YFP FRET) are indicated (red sticks); among these mutations, Leu416Ser/Leu423Ser within OASF spontaneously induces maximum CRAC currents (Muik et al., 2011). (B) Dimer unit observed in the *D. melanogaster* Orai hexameric crystal structure (4HKR.pdb). Each monomer is shaded a different shade of gray. The antiparallel coiled-coil (broken black box) which forms in the CTD of each dimer unit is colored yellow. The hydrophobic residues (purple sticks) involved in stabilizing the coiled-coil and the dimer unit are indicated. All structure images were rendered in PyMOL.

sequence divergence in the intracellular N- and C-terminal regions of the human Orai homologues contribute to the functional differences of the Orai channels (Frischauf et al., 2009); however, as per the STIM proteins, other regions of poor sequence conservation among the human Orai proteins may also play a role in dictating functional variation.

Recently, an X-ray crystal structure of the *D. melanogaster* Orai channel in the closed state has provided some high-resolution information on potential mechanisms of interaction with STIM molecules (Hou et al., 2012). Surprisingly, the *D. melanogaster* Orai channel crystallized in a hexameric state; moreover, this is in contrast to studies suggesting that human Orai1 is an active tetramer (Ji et al., 2008; Madl et al., 2010; Maruyama et al., 2009; Penna et al., 2008). The hexameric Orai structure exhibits a threefold symmetry on the outer region as the C-terminal domain adopts two different conformations, whereas TM1 from the six subunits forms the inner ring of the channel and the pore with a sixfold axis of symmetry. The TM1-assembled pore is comprised of a ring of glutamates (i.e., Glu178, corresponding to human Glu106) near the extracellular surface, a hydrophobic region (i.e., Val174, Phe171, and Leu167, corresponding to human Val102, Phe99, and Leu95), and a basic stretch near the intracellular side of the pore (i.e., Lys163, Lys159, and Arg155, corresponding to human Arg91, Lys87, and Arg83). Ca^{2+} binding occurs at the glutamate ring, and interestingly, anion binding was discovered at the basic region of the pore, although the identity of the anion is not certain. Remarkably, the C-terminal regions of two Orai subunits interact, creating a minimal dimer unit which is repeated three times in the hexameric architecture (Fig. 3.5B). The cytosolic C-terminal domains from two subunits of Orai form an antiparallel CC interaction, where Ile316 packs against Leu319 from the opposite subunit and vice versa. Considering the putative CC nature of the STIM cytosolic domains, it is tempting to speculate that this C-terminal region of the dimer unit represents a STIM attachment domain, colocalizing via a STIM:Orai CC interaction mechanism.

9. CONCLUDING REMARKS

The high-resolution structural data on the EF–SAM region of STIM1 and STIM2, the SOAR domain of STIM1 and *C. elegans* STIM, and the *D. melanogaster* Orai hexamer channel structure have revealed a remarkable breadth of mechanistic data on how STIM and Orai proteins create CRAC channels. In the case of the EF–SAM domains, the intimate interaction between the EF-hand and SAM domains keeps STIM molecules in a

quiescent state and maintains SOCE in an OFF state. Moreover, the "open" EF-hand conformation facilitates the robust hydrophobic packing when Ca^{2+} is bound in the canonical EF-hand. ER luminal Ca^{2+} depletion results in a drastic destabilization of this EF-hand:SAM interaction, promoting oligomerization of EF–SAM. The EF–SAM oligomerization initiates downstream mechanistic steps involved in CRAC channel activation. One such step that has been experimentally exposed is a conformational transition which must occur to the cytosolic domains of STIM prior to Orai recruitment and channel gating. This conformational change involves SOAR, which X-ray crystal structures have shown may be in an inhibited state through interactions with a region of CC1. Finally, the *D. melanogaster* Orai hexamer structure has revealed that individual Orai dimer units are repeated in the higher order hexamer structure of the channel as well as the precise composition of the closed channel pore which includes an anion binding site near the intracellular channel opening. The Orai dimer units are stabilized by antiparallel CC interactions between the cytosolic C-terminal domains of each Orai subunit, and this antiparallel intersubunit CC region may represent a recruiting handle for STIM proteins.

Despite progress in illuminating important structural features of the CRAC channel complex, several structural milestones regarding the activation mechanism remain elusive. First, how does the EF–SAM oligomerization transmit a signal to the CC domains that induces cytosolic domain oligomerization? Second, how does the SOAR region of STIM interact with the C-terminal antiparallel CC domain within each dimer unit of Orai? Third, what structural changes occur within SOAR to promote and mediate the Orai recruitment via these C-terminal domains? Fourth, what structural alterations occur to the Orai C-terminal CC region upon complexation with SOAR and are these conformational changes also involved in channel gating? Fifth, how does the Orai N-terminal region interact with SOAR and how does this interaction propagate CRAC channel pore gating through a TM1 conformational change? Sixth, what is the structural basis for oligomerization of the cytosolic region of STIM? Finally, what is the "open" CRAC channel complex stoichiometry (i.e., number of STIM relative to number of Orai molecules). The answer to these structural questions combined with the structural data garnered to date will provide a basis to the development of new strategies for the maintenance of human health as well as development of therapeutics which act in the SOCE pathway to modulate Ca^{2+} signaling and treat Ca^{2+}-signaling-mediated malignancies.

ACKNOWLEDGMENTS

This work was made possible through CIHR, HSFC, NSERC, and CFI funding to M. I. M. I. holds the Canada Research Chain in Cancer structural biology.

REFERENCES

Baba, Y., Hayashi, K., Fujii, Y., Mizushima, A., Watarai, H., Wakamori, M., et al. (2006). Coupling of STIM1 to store-operated Ca^{2+} entry through its constitutive and inducible movement in the endoplasmic reticulum. *Proceedings of the National Academy of Sciences of the United States of America*, *103*(45), 16704–16709.

Baker, N. A., Sept, D., Joseph, S., Holst, M. J., & McCammon, J. A. (2001). Electrostatics of nanosystems: Application to microtubules and the ribosome. *Proceedings of the National Academy of Sciences of the United States of America*, *98*(18), 10037–10041.

Berridge, M. J. (2002). The endoplasmic reticulum: A multifunctional signaling organelle. *Cell Calcium*, *32*(5–6), 235–249.

Berridge, M. J., Bootman, M. D., & Roderick, H. L. (2003). Calcium signalling: Dynamics, homeostasis and remodelling. *Nature Reviews. Molecular Cell Biology*, *4*(7), 517–529.

Berridge, M. J., Lipp, P., & Bootman, M. D. (2000). The versatility and universality of calcium signalling. *Nature Reviews. Molecular Cell Biology*, *1*(1), 11–21.

Bogeski, I., Al-Ansary, D., Qu, B., Niemeyer, B. A., Hoth, M., & Peinelt, C. (2010). Pharmacology of ORAI channels as a tool to understand their physiological functions. *Expert Review of Clinical Pharmacology*, *3*(3), 291–303.

Bootman, M. D., Collins, T. J., Peppiatt, C. M., Prothero, L. S., MacKenzie, L., De Smet, P., et al. (2001). Calcium signalling—An overview. *Seminars in Cell & Developmental Biology*, *12*(1), 3–10.

Bootman, M. D., & Lipp, P. (2001). Calcium signalling and regulation of cell function. *Encyclopedia of Life Sciences*, 1–7.

Brandman, O., Liou, J., Park, W. S., & Meyer, T. (2007). STIM2 is a feedback regulator that stabilizes basal cytosolic and endoplasmic reticulum Ca^{2+} levels. *Cell*, *131*(7), 1327–1339.

Byun, M., Abhyankar, A., Lelarge, V., Plancoulaine, S., Palanduz, A., Telhan, L., et al. (2010). Whole-exome sequencing-based discovery of STIM1 deficiency in a child with fatal classic Kaposi sarcoma. *The Journal of Experimental Medicine*, *207*(11), 2307–2312.

Cai, X. (2007a). Molecular evolution and functional divergence of the Ca(2+) sensor protein in store-operated Ca(2+) entry: Stromal interaction molecule. *PLoS One*, *2*(7), e609.

Cai, X. (2007b). Molecular evolution and structural analysis of the Ca(2+) release-activated Ca(2+) channel subunit, Orai. *Journal of Molecular Biology*, *368*(5), 1284–1291.

Calloway, N., Owens, T., Corwith, K., Rodgers, W., Holowka, D., & Baird, B. (2011). Stimulated association of STIM1 and Orai1 is regulated by the balance of PtdIns(4,5)P(2) between distinct membrane pools. *Journal of Cell Science*, *124*(Pt. 15), 2602–2610.

Capiod, T. (2012). Immunodeficiencies and pathologies associated with mutations in STIM/Orai. Available from: http://hstalks.com/bio.

Covington, E. D., Wu, M. M., & Lewis, R. S. (2010). Essential role for the CRAC activation domain in store-dependent oligomerization of STIM1. *Molecular Biology of the Cell*, *21*(11), 1897–1907.

Darbellay, B., Arnaudeau, S., Bader, C. R., Konig, S., & Bernheim, L. (2012). STIM1L is a new actin-binding splice variant involved in fast repetitive Ca^{2+} release. *The Journal of Cell Biology*, *194*(2), 335–346.

DeHaven, W. I., Smyth, J. T., Boyles, R. R., & Putney, J. W., Jr. (2007). Calcium inhibition and calcium potentiation of Orai1, Orai2, and Orai3 calcium release-activated calcium channels. *The Journal of Biological Chemistry*, *282*(24), 17548–17556.

Derler, I., Fahrner, M., Muik, M., Lackner, B., Schindl, R., Groschner, K., et al. (2009). A CRAC modulatory domain (CMD) within STIM1 mediates fast Ca^{2+}-dependent inactivation of ORAI1 channels. *The Journal of Biological Chemistry*, *284*(37), 24933–24938.

Dolinsky, T. J., Czodrowski, P., Li, H., Nielsen, J. E., Jensen, J. H., Klebe, G., et al. (2007). PDB2PQR: Expanding and upgrading automated preparation of biomolecular structures for molecular simulations. *Nucleic Acids Research*, *35*(Web Server issue), W522–W525.

Draber, P., & Draberova, L. (2005). Lifting the fog in store-operated Ca^{2+} entry. *Trends in Immunology*, *26*(12), 621–624.

Faouzi, M., Hague, F., Potier, M., Ahidouch, A., Sevestre, H., & Ouadid-Ahidouch, H. (2011). Down-regulation of Orai3 arrests cell-cycle progression and induces apoptosis in breast cancer cells but not in normal breast epithelial cells. *Journal of Cellular Physiology*, *226*(2), 542–551.

Faouzi, M., Kischel, P., Hague, F., Ahidouch, A., Benzerdjeb, N., Sevestre, H., et al. (2013). ORAI3 silencing alters cell proliferation and cell cycle progression via c-myc pathway in breast cancer cells. *Biochimica et Biophysica Acta*, *1833*(3), 752–760.

Feske, S. (2007). Calcium signalling in lymphocyte activation and disease. *Nature Reviews Immunology*, *7*(9), 690–702.

Feske, S. (2012). Immunodeficiency due to defects in store-operated calcium entry. *Annals of the New York Academy of Sciences*, *1238*, 74–90.

Feske, S., Gwack, Y., Prakriya, M., Srikanth, S., Puppel, S. H., Tanasa, B., et al. (2006). A mutation in Orai1 causes immune deficiency by abrogating CRAC channel function. *Nature*, *441*(7090), 179–185.

Feske, S., Skolnik, E. Y., & Prakriya, M. (2012). Ion channels and transporters in lymphocyte function and immunity. *Nature Reviews. Immunology*, *12*(7), 532–547.

Frischauf, I., Muik, M., Derler, I., Bergsmann, J., Fahrner, M., Schindl, R., et al. (2009). Molecular determinants of the coupling between STIM1 and Orai channels: Differential activation of Orai1-3 channels by a STIM1 coiled-coil mutant. *The Journal of Biological Chemistry*, *284*(32), 21696–21706.

Frischauf, I., Schindl, R., Bergsmann, J., Derler, I., Fahrner, M., Muik, M., et al. (2011). Cooperativeness of Orai cytosolic domains tunes subtype-specific gating. *The Journal of Biological Chemistry*, *286*(10), 8577–8584.

Fuchs, S., Rensing-Ehl, A., Speckmann, C., Bengsch, B., Schmitt-Graeff, A., Bondzio, I., et al. (2012). Antiviral and regulatory T cell immunity in a patient with stromal interaction molecule 1 deficiency. *Journal of Immunology*, *188*(3), 1523–1533.

Gao, S., Fan, Y., Chen, L., Lu, J., Xu, T., & Xu, P. (2009). Mechanism of different spatial distributions of *Caenorhabditis elegans* and human STIM1 at resting state. *Cell Calcium*, *45*(1), 77–88.

Gifford, J. L., Walsh, M. P., & Vogel, H. J. (2007). Structures and metal-ion-binding properties of the Ca^{2+}-binding helix-loop-helix EF-hand motifs. *The Biochemical Journal*, *405*(2), 199–221.

Graham, S. J., Dziadek, M. A., & Johnstone, L. S. (2011). A cytosolic STIM2 preprotein created by signal peptide inefficiency activates ORAI1 in a store-independent manner. *The Journal of Biological Chemistry*, *286*(18), 16174–16185.

Gwack, Y., Srikanth, S., Feske, S., Cruz-Guilloty, F., Oh-hora, M., Neems, D. S., et al. (2007). Biochemical and functional characterization of Orai proteins. *The Journal of Biological Chemistry*, *282*(22), 16232–16243.

Hogan, P. G., Chen, L., Nardone, J., & Rao, A. (2003). Transcriptional regulation by calcium, calcineurin, and NFAT. *Genes & Development*, *17*(18), 2205–2232.

Horinouchi, T., Higashi, T., Higa, T., Terada, K., Mai, Y., Aoyagi, H., et al. (2012). Different binding property of STIM1 and its novel splice variant STIM1L to Orai1, TRPC3, and TRPC6 channels. *Biochemical and Biophysical Research Communications*, *428*(2), 252–258.

Hou, X., Pedi, L., Diver, M. M., & Long, S. B. (2012). Crystal structure of the calcium release-activated calcium channel Orai. *Science*, *338*(6112), 1308–1313.

Huang, X., & Miller, W. (1991). A time-efficient, linear-space local similarity algorithm. *Advances in Applied Mathematics*, *12*, 373–381.

Huang, Y., Zhou, Y., Wong, H. C., Chen, Y., Wang, S., Castiblanco, A., et al. (2009). A single EF-hand isolated from STIM1 forms dimer in the absence and presence of Ca^{2+}. *The FEBS Journal*, *276*(19), 5589–5597.

Ikura, M., & Ames, J. B. (2006). Genetic polymorphism and protein conformational plasticity in the calmodulin superfamily: Two ways to promote multifunctionality. *Proceedings of the National Academy of Sciences of the United States of America*, *103*(5), 1159–1164.

Jackson, T. R., Patterson, S. I., Thastrup, O., & Hanley, M. R. (1988). A novel tumour promoter, thapsigargin, transiently increases cytoplasmic free Ca^{2+} without generation of inositol phosphates in NG115-401L neuronal cells. *The Biochemical Journal*, *253*(1), 81–86.

Ji, W., Xu, P., Li, Z., Lu, J., Liu, L., Zhan, Y., et al. (2008). Functional stoichiometry of the unitary calcium-release-activated calcium channel. *Proceedings of the National Academy of Sciences of the United States of America*, *105*(36), 13668–13673.

Kawasaki, T., Lange, I., & Feske, S. (2009). A minimal regulatory domain in the C terminus of STIM1 binds to and activates ORAI1 CRAC channels. *Biochemical and Biophysical Research Communications*, *385*(1), 49–54.

Kim, C. A., & Bowie, J. U. (2003). SAM domains: Uniform structure, diversity of function. *Trends in Biochemical Sciences*, *28*(12), 625–628.

Korzeniowski, M. K., Manjarres, I. M., Varnai, P., & Balla, T. (2011). Activation of STIM1–Orai1 involves an intramolecular switching mechanism. *Science Signaling*, *3*(148), ra82.

Korzeniowski, M. K., Popovic, M. A., Szentpetery, Z., Varnai, P., Stojilkovic, S. S., & Balla, T. (2009). Dependence of STIM1/Orai1-mediated calcium entry on plasma membrane phosphoinositides. *The Journal of Biological Chemistry*, *284*(31), 21027–21035.

Koveal, D., Schuh-Nuhfer, N., Ritt, D., Page, R., Morrison, D. K., & Peti, W. (2012). A CC-SAM, for coiled coil-sterile alpha motif, domain targets the scaffold KSR-1 to specific sites in the plasma membrane. *Science Signaling*, *5*(255), ra94.

Lawrence, R. J. (1985). David the "Bubble Boy" and the boundaries of the human. *JAMA: The Journal of the American Medical Association*, *253*(1), 74–76.

Le Deist, F., Hivroz, C., Partiseti, M., Thomas, C., Buc, H. A., Oleastro, M., et al. (1995). A primary T-cell immunodeficiency associated with defective transmembrane calcium influx. *Blood*, *85*(4), 1053–1062.

Liou, J., Fivaz, M., Inoue, T., & Meyer, T. (2007). Live-cell imaging reveals sequential oligomerization and local plasma membrane targeting of stromal interaction molecule 1 after Ca^{2+} store depletion. *Proceedings of the National Academy of Sciences of the United States of America*, *104*(22), 9301–9306.

Liou, J., Kim, M. L., Heo, W. D., Jones, J. T., Myers, J. W., Ferrell, J. E., Jr., et al. (2005). STIM is a Ca^{2+} sensor essential for Ca^{2+}-store-depletion-triggered Ca^{2+} influx. *Current Biology*, *15*(13), 1235–1241.

Lis, A., Peinelt, C., Beck, A., Parvez, S., Monteilh-Zoller, M., Fleig, A., et al. (2007). CRACM1, CRACM2, and CRACM3 are store-operated Ca^{2+} channels with distinct functional properties. *Current Biology*, *17*(9), 794–800.

Lorin-Nebel, C., Xing, J., Yan, X., & Strange, K. (2007). CRAC channel activity in *C. elegans* is mediated by Orai1 and STIM1 homologues and is essential for ovulation and fertility. *The Journal of Physiology*, *580*(Pt. 1), 67–85.

Luik, R. M., Wang, B., Prakriya, M., Wu, M. M., & Lewis, R. S. (2008). Oligomerization of STIM1 couples ER calcium depletion to CRAC channel activation. *Nature*, *454*(7203), 538–542.

Luik, R. M., Wu, M. M., Buchanan, J., & Lewis, R. S. (2006). The elementary unit of store-operated Ca^{2+} entry: Local activation of CRAC channels by STIM1 at ER-plasma membrane junctions. *The Journal of Cell Biology*, *174*(6), 815–825.

Madl, J., Weghuber, J., Fritsch, R., Derler, I., Fahrner, M., Frischauf, I., et al. (2010). Resting state Orai1 diffuses as homotetramer in the plasma membrane of live mammalian cells. *The Journal of Biological Chemistry*, *285*(52), 41135–41142.

Manji, S. S., Parker, N. J., Williams, R. T., van Stekelenburg, L., Pearson, R. B., Dziadek, M., et al. (2000). STIM1: A novel phosphoprotein located at the cell surface. *Biochimica et Biophysica Acta*, *1481*(1), 147–155.

Maruyama, Y., Ogura, T., Mio, K., Kato, K., Kaneko, T., Kiyonaka, S., et al. (2009). Tetrameric Orai1 is a teardrop-shaped molecule with a long, tapered cytoplasmic domain. *The Journal of Biological Chemistry*, *284*(20), 13676–13685.

McAndrew, D., Grice, D. M., Peters, A. A., Davis, F. M., Stewart, T., Rice, M., et al. (2011). ORAI1-mediated calcium influx in lactation and in breast cancer. *Molecular Cancer Therapeutics*, *10*(3), 448–460.

McNally, B. A., & Prakriya, M. (2012). Permeation, selectivity, and gating in store-operated CRAC channels. *The Journal of Physiology*, *590*(Pt. 17), 4179–4191.

McNally, B. A., Somasundaram, A., Yamashita, M., & Prakriya, M. (2012). Gated regulation of CRAC channel ion selectivity by STIM1. *Nature*, *482*(7384), 241–245.

McNally, B. A., Yamashita, M., Engh, A., & Prakriya, M. (2009). Structural determinants of ion permeation in CRAC channels. *Proceedings of the National Academy of Sciences of the United States of America*, *106*(52), 22516–22521.

Mercer, J. C., Dehaven, W. I., Smyth, J. T., Wedel, B., Boyles, R. R., Bird, G. S., et al. (2006). Large store-operated calcium-selective currents due to co-expression of Orai1 or Orai2 with the intracellular calcium sensor, Stim1. *The Journal of Biological Chemistry*, *281*(34), 24979–24990.

Mignen, O., Thompson, J. L., & Shuttleworth, T. J. (2008). Orai1 subunit stoichiometry of the mammalian CRAC channel pore. *The Journal of Physiology*, *586*(2), 419–425.

Motiani, R. K., Abdullaev, I. F., & Trebak, M. (2010). A novel native store-operated calcium channel encoded by Orai3: Selective requirement of Orai3 versus Orai1 in estrogen receptor-positive versus estrogen receptor-negative breast cancer cells. *The Journal of Biological Chemistry*, *285*(25), 19173–19183.

Motiani, R. K., Zhang, X., Harmon, K. E., Keller, R. S., Matrougui, K., Bennett, J. A., et al. (2013). Orai3 is an estrogen receptor alpha-regulated Ca^{2+} channel that promotes tumorigenesis. *The FASEB Journal*, *27*(1), 63–75.

Muik, M., Fahrner, M., Derler, I., Schindl, R., Bergsmann, J., Frischauf, I., et al. (2009). A cytosolic homomerization and a modulatory domain within STIM1 C terminus determine coupling to ORAI1 channels. *The Journal of Biological Chemistry*, *284*(13), 8421–8426.

Muik, M., Fahrner, M., Schindl, R., Stathopulos, P., Frischauf, I., Derler, I., et al. (2011). STIM1 couples to ORAI1 via an intramolecular transition into an extended conformation. *The EMBO Journal*, *30*(9), 1678–1689.

Muik, M., Frischauf, I., Derler, I., Fahrner, M., Bergsmann, J., Eder, P., et al. (2008). Dynamic coupling of the putative coiled-coil domain of ORAI1 with STIM1 mediates ORAI1 channel activation. *The Journal of Biological Chemistry*, *283*(12), 8014–8022.

Muik, M., Schindl, R., Fahrner, M., & Romanin, C. (2012). Ca(2+) release-activated Ca(2+) (CRAC) current, structure, and function. *Cellular and Molecular Life Sciences*, *69*(24), 4163–4176.

Parekh, A. B., & Penner, R. (1997). Store depletion and calcium influx. *Physiological Reviews*, *77*(4), 901–930.

Parekh, A. B., & Putney, J. W., Jr. (2005). Store-operated calcium channels. *Physiological Reviews*, *85*(2), 757–810.

Park, C. Y., Hoover, P. J., Mullins, F. M., Bachhawat, P., Covington, E. D., Raunser, S., et al. (2009). STIM1 clusters and activates CRAC channels via direct binding of a cytosolic domain to Orai1. *Cell*, *136*(5), 876–890.

Partiseti, M., Le Deist, F., Hivroz, C., Fischer, A., Korn, H., & Choquet, D. (1994). The calcium current activated by T cell receptor and store depletion in human lymphocytes is absent in a primary immunodeficiency. *The Journal of Biological Chemistry*, *269*(51), 32327–32335.

Penna, A., Demuro, A., Yeromin, A. V., Zhang, S. L., Safrina, O., Parker, I., et al. (2008). The CRAC channel consists of a tetramer formed by Stim-induced dimerization of Orai dimers. *Nature*, *456*(7218), 116–120.

Picard, C., McCarl, C. A., Papolos, A., Khalil, S., Luthy, K., Hivroz, C., et al. (2009). STIM1 mutation associated with a syndrome of immunodeficiency and autoimmunity. *The New England Journal of Medicine*, *360*(19), 1971–1980.

Prakriya, M., Feske, S., Gwack, Y., Srikanth, S., Rao, A., & Hogan, P. G. (2006). Orai1 is an essential pore subunit of the CRAC channel. *Nature*, *443*(7108), 230–233.

Putney, J. W., Jr. (1986). A model for receptor-regulated calcium entry. *Cell Calcium*, 7(1), 1–12.

Roos, J., DiGregorio, P. J., Yeromin, A. V., Ohlsen, K., Lioudyno, M., Zhang, S., et al. (2005). STIM1, an essential and conserved component of store-operated Ca^{2+} channel function. *The Journal of Cell Biology*, *169*(3), 435–445.

Schindl, R., Frischauf, I., Bergsmann, J., Muik, M., Derler, I., Lackner, B., et al. (2009). Plasticity in Ca^{2+} selectivity of Orai1/Orai3 heteromeric channel. *Proceedings of the National Academy of Sciences of the United States of America*, *106*(46), 19623–19628.

Seo, M. D., Velamakanni, S., Ishiyama, N., Stathopulos, P. B., Rossi, A. M., Khan, S. A., et al. (2012). Structural and functional conservation of key domains in InsP3 and ryanodine receptors. *Nature*, *483*(7387), 108–112.

Shaw, P. J., & Feske, S. (2012). Physiological and pathophysiological functions of SOCE in the immune system. *Frontiers in Bioscience (Elite Edition)*, *4*, 2253–2268.

Sievers, F., Wilm, A., Dineen, D., Gibson, T. J., Karplus, K., Li, W., et al. (2011). Fast, scalable generation of high-quality protein multiple sequence alignments using Clustal Omega. *Molecular Systems Biology*, *7*, 539.

Soboloff, J., Spassova, M. A., Tang, X. D., Hewavitharana, T., Xu, W., & Gill, D. L. (2006). Orai1 and STIM reconstitute store-operated calcium channel function. *The Journal of Biological Chemistry*, *281*(30), 20661–20665.

Stathopulos, P. B., Li, G. Y., Plevin, M. J., Ames, J. B., & Ikura, M. (2006). Stored Ca^{2+} depletion-induced oligomerization of stromal interaction molecule 1 (STIM1) via the EF-SAM region: An initiation mechanism for capacitive Ca^{2+} entry. *The Journal of Biological Chemistry*, *281*(47), 35855–35862.

Stathopulos, P. B., Seo, M. D., Enomoto, M., Amador, F. J., Ishiyama, N., & Ikura, M. (2012). Themes and variations in ER/SR calcium release channels: Structure and function. *Physiology (Bethesda, MD)*, *27*(6), 331–342.

Stathopulos, P. B., Zheng, L., & Ikura, M. (2009). Stromal interaction molecule (STIM) 1 and STIM2 calcium sensing regions exhibit distinct unfolding and oligomerization kinetics. *The Journal of Biological Chemistry*, *284*(2), 728–732.

Stathopulos, P. B., Zheng, L., Li, G. Y., Plevin, M. J., & Ikura, M. (2008). Structural and mechanistic insights into STIM1-mediated initiation of store-operated calcium entry. *Cell*, *135*(1), 110–122.

Stone, B. (1977). The 'boy-in-the-bubble' drama. *American Medical News*, *20*(46), 1+.

Thompson, J. L., Mignen, O., & Shuttleworth, T. J. (2009). The Orai1 severe combined immune deficiency mutation and calcium release-activated Ca^{2+} channel function in the heterozygous condition. *The Journal of Biological Chemistry*, *284*(11), 6620–6626.

Van Petegem, F. (2012). Ryanodine receptors: Structure and function. *The Journal of Biological Chemistry*, *287*(38), 31624–31632.

Varga-Szabo, D., Braun, A., & Nieswandt, B. (2009). Calcium signaling in platelets. *Journal of Thrombosis and Haemostasis*, *7*(7), 1057–1066.
Varga-Szabo, D., Braun, A., & Nieswandt, B. (2011). STIM and Orai in platelet function. *Cell Calcium*, *50*(3), 270–278.
Varnai, P., Toth, B., Toth, D. J., Hunyady, L., & Balla, T. (2007). Visualization and manipulation of plasma membrane-endoplasmic reticulum contact sites indicates the presence of additional molecular components within the STIM1–Orai1 Complex. *The Journal of Biological Chemistry*, *282*(40), 29678–29690.
Vig, M., Beck, A., Billingsley, J. M., Lis, A., Parvez, S., Peinelt, C., et al. (2006). CRACM1 multimers form the ion-selective pore of the CRAC channel. *Current Biology*, *16*(20), 2073–2079.
Vig, M., Peinelt, C., Beck, A., Koomoa, D. L., Rabah, D., Koblan-Huberson, M., et al. (2006). CRACM1 is a plasma membrane protein essential for store-operated Ca^{2+} entry. *Science*, *312*(5777), 1220–1223.
Walsh, C. M., Chvanov, M., Haynes, L. P., Petersen, O. H., Tepikin, A. V., & Burgoyne, R. D. (2010). Role of phosphoinositides in STIM1 dynamics and store-operated calcium entry. *The Biochemical Journal*, *425*(1), 159–168.
Williams, R. T., Manji, S. S., Parker, N. J., Hancock, M. S., Van Stekelenburg, L., Eid, J. P., et al. (2001). Identification and characterization of the STIM (stromal interaction molecule) gene family: Coding for a novel class of transmembrane proteins. *The Biochemical Journal*, *357*(Pt. 3), 673–685.
Williams, R. T., Senior, P. V., Van Stekelenburg, L., Layton, J. E., Smith, P. J., & Dziadek, M. A. (2002). Stromal interaction molecule 1 (STIM1), a transmembrane protein with growth suppressor activity, contains an extracellular SAM domain modified by N-linked glycosylation. *Biochimica et Biophysica Acta*, *1596*(1), 131–137.
Wu, M. M., Buchanan, J., Luik, R. M., & Lewis, R. S. (2006). Ca^{2+} store depletion causes STIM1 to accumulate in ER regions closely associated with the plasma membrane. *The Journal of Cell Biology*, *174*(6), 803–813.
Xu, P., Lu, J., Li, Z., Yu, X., Chen, L., & Xu, T. (2006). Aggregation of STIM1 underneath the plasma membrane induces clustering of Orai1. *Biochemical and Biophysical Research Communications*, *350*(4), 969–976.
Yan, X., Xing, J., Lorin-Nebel, C., Estevez, A. Y., Nehrke, K., Lamitina, T., et al. (2006). Function of a STIM1 homologue in *C. elegans*: Evidence that store-operated Ca^{2+} entry is not essential for oscillatory Ca^{2+} signaling and ER Ca^{2+} homeostasis. *The Journal of General Physiology*, *128*(4), 443–459.
Yang, X., Jin, H., Cai, X., Li, S., & Shen, Y. (2012). Structural and mechanistic insights into the activation of Stromal interaction molecule 1 (STIM1). *Proceedings of the National Academy of Sciences of the United States of America*, *109*(15), 5657–5662.
Yeromin, A. V., Zhang, S. L., Jiang, W., Yu, Y., Safrina, O., & Cahalan, M. D. (2006). Molecular identification of the CRAC channel by altered ion selectivity in a mutant of Orai. *Nature*, *443*(7108), 226–229.
Yuan, J. P., Zeng, W., Dorwart, M. R., Choi, Y. J., Worley, P. F., & Muallem, S. (2009). SOAR and the polybasic STIM1 domains gate and regulate Orai channels. *Nature Cell Biology*, *11*(3), 337–343.
Zhang, W., & Trebak, M. (2011). STIM1 and Orai1: Novel targets for vascular diseases? *Science China. Life Sciences*, *54*(8), 780–785.
Zhang, S. L., Yeromin, A. V., Hu, J., Amcheslavsky, A., Zheng, H., & Cahalan, M. D. (2011). Mutations in Orai1 transmembrane segment 1 cause STIM1-independent activation of Orai1 channels at glycine 98 and channel closure at arginine 91. *Proceedings of the National Academy of Sciences of the United States of America*, *108*(43), 17838–17843.
Zhang, S. L., Yeromin, A. V., Zhang, X. H., Yu, Y., Safrina, O., Penna, A., et al. (2006). Genome-wide RNAi screen of Ca(2+) influx identifies genes that regulate Ca(2+)

release-activated Ca(2+) channel activity. *Proceedings of the National Academy of Sciences of the United States of America*, *103*(24), 9357–9362.

Zhang, S. L., Yu, Y., Roos, J., Kozak, J. A., Deerinck, T. J., Ellisman, M. H., et al. (2005). STIM1 is a Ca^{2+} sensor that activates CRAC channels and migrates from the Ca^{2+} store to the plasma membrane. *Nature*, *437*(7060), 902–905.

Zheng, L., Stathopulos, P. B., Li, G. Y., & Ikura, M. (2008). Biophysical characterization of the EF-hand and SAM domain containing Ca^{2+} sensory region of STIM1 and STIM2. *Biochemical and Biophysical Research Communications*, *369*(1), 240–246.

Zheng, L., Stathopulos, P. B., Schindl, R., Li, G. Y., Romanin, C., & Ikura, M. (2011). Auto-inhibitory role of the EF-SAM domain of STIM proteins in store-operated calcium entry. *Proceedings of the National Academy of Sciences of the United States of America*, *108*(4), 1337–1342.

Zhou, Y., Mancarella, S., Wang, Y., Yue, C., Ritchie, M., Gill, D. L., et al. (2009). The short N-terminal domains of STIM1 and STIM2 control the activation kinetics of Orai1 channels. *The Journal of Biological Chemistry*, *284*(29), 19164–19168.

Zhou, Y., Meraner, P., Kwon, H. T., Machnes, D., Oh-hora, M., Zimmer, J., et al. (2010). STIM1 gates the store-operated calcium channel ORAI1 in vitro. *Nature Structural & Molecular Biology*, *17*(1), 112–116.

Zhou, Y., Ramachandran, S., Oh-Hora, M., Rao, A., & Hogan, P. G. (2010). Pore architecture of the ORAI1 store-operated calcium channel. *Proceedings of the National Academy of Sciences of the United States of America*, *107*(11), 4896–4901.